Electronic Supplementary Material (ESI) for RSC Advances.

Stepwise dissolution and composition determination of samples of multiple crystals using a dissolution medium containing aqueous alcohol and fluorocarbon phases.

Humphrey A. Moynihan and Declan Armstrong

SUPPLEMENTARY INFORMATION

Contents

Synthetic Procedures
Synthesis of 2-nitro-4-*tert*-butylacetanilide (3): page 3
Fig. S1. Chemical structure of 2-nitro-4-*t*-butylacetanilide **(3)**: page 3

NMR Spectra
Fig. S2. ^{1}H NMR spectrum of **3**: page 4
Fig. S3. ^{13}C NMR spectrum of **3**: page 4
Fig. S4. ^{19}F NMR spectrum of **4**: page 5
Fig. S5. ^{1}H NMR spectrum of **4**: page 5
Fig. S6. ^{19}F NMR spectra of **4**: page 6

HPLC Calibration Data: page 7

Particle Sizing: page 11
Fig. S7. An image highlighting the typical perimeter established for area measurements and the typical dimension established for length measurements.

Impurity incorporation: page 12
Fig. S8. Graph displaying incorporation level versus solution impurity level of 4-methyl-2-nitroacetanilide (**2**) in "host" crystals of 4-trifluoromethyl-2-nitroacetanilide.
Table S1. Overall incorporation (% composition by HPLC) of 4-methyl-2-nitroacetanilide (**2**) and 4-*tert*-butyl-2-nitroacetanilide (**3**) in crystals of 4-chloro-2-nitroacetanilide (**1**) obtained by crystallisation from solutions in toluene containing various quantities of **2** and **3** at a σ value of 1.5. Data is shown for two crystallisation batches.

Powder X-ray Diffraction: page 14
Fig. S9. Powder X-ray diffraction patterns obtained for crystals of **1** grown from toluene, **1** grown from toluene with concentrations of 5 mol% **2**, and **2** grown from toluene: page 14
Fig. S10. Powder X-ray diffraction patterns obtained for crystals of **1** grown from toluene, **1** grown from toluene with concentrations of 4.5 mol % **3**, and **3** grown from toluene: page 15

Differential Scanning Calorimetry: page 16
Fig. S11. DSC curves obtained from crystals of **1** containing 5 mol % **2**; compared to DSC curves of component compound **1** and compound **2**: page 16
Fig. S12. DSC curves obtained from crystals of **1** containing 4.5 mol % **3**; compared to DSC curves of component compound **1** and compound **3**: page 16

Partial Dissolution Graphs: page 17

Fig. S13. Chart comparing particle area versus the ranking of each particle in a partial dissolution series of **1** doped with 1.5 mol % of **2**: page 17
Fig. S14. Chart comparing particle length versus the ranking of each particle in a partial dissolution series of **1** doped with 1.5 mol % of **2**: page 17
Fig. S15. Plot of percentage by HPLC of added impurity in crystals of compound **1** *vs.* the dissolution mid-point for the sample of crystals grown from solutions containing 1.5 mol % of additive **2**: page 17
Fig. S16. Chart comparing particle area versus the ranking of each particle in a partial dissolution series of **1** doped with 2.0 mol % of **2**: page 18
Fig. S17. Chart comparing particle length versus the ranking of each particle in a partial dissolution series of **1** doped with 2.0 mol % of **2**: page 19
Fig. S18. Plot of percentage by HPLC of added impurity in crystals of compound **1** *vs.* the dissolution mid-point for the sample of crystals grown from solutions containing 2.0 mol % of additive **2**: page 19
Fig. S19. Chart comparing particle area versus the ranking of each particle in a partial dissolution series of **1** doped with 2.5 mol % of **2**: page 20
Fig. S20. Chart comparing particle length versus the ranking of each particle in a partial dissolution series of **1** doped with 2.5 mol % of **2**: page 20
Fig. S21. Plot of percentage by HPLC of added impurity in crystals of compound **1** *vs.* the dissolution mid-point for the sample of crystals grown from solutions containing 2.5 mol % of additive **2**: page 21
Fig. S22. Chart comparing particle area versus the ranking of each particle in a partial dissolution series of **1** doped with 3.0 mol % of **2**: page 21
Fig. S23. Chart comparing particle length versus the ranking of each particle in a partial dissolution series of **1** doped with 3.0 mol % of **2**: page 22
Fig. S24. Plot of percentage by HPLC of added impurity in crystals of compound **1** *vs.* the dissolution mid-point for the sample of crystals grown from solutions containing 3.0 mol % of additive **2**: page 22
Fig. S25. Chart comparing particle area versus the ranking of each particle in a partial dissolution series of **1** doped with 3.5 mol % of **2**: page 23
Fig. S26. Chart comparing particle length versus the ranking of each particle in a partial dissolution series of **1** doped with 3.5 mol % of **2**: page 23
Fig. S27. Plot of percentage by HPLC of added impurity in crystals of compound **1** *vs.* the dissolution mid-point for the sample of crystals grown from solutions containing 3.5 mol % of additive **2**: page 24
Fig. S28. Chart comparing particle area versus the ranking of each particle in a partial dissolution series of 1 doped with 4.0 mol % of 2: page 24
Fig. S29. Chart comparing particle length versus the ranking of each particle in a partial dissolution series of 1 doped with 4.0 mol % of 2: page 25
Fig. S30. Plot of percentage by HPLC of added impurity in crystals of compound **1** *vs.* the dissolution mid-point for the sample of crystals grown from solutions containing 4.0 mol % of additive **2**: page 25
Fig. S21. Chart comparing particle area versus the ranking of each particle in a partial dissolution series of **1** doped with 4.5 mol % of **2**: page 26
Fig. S32. Chart comparing particle length versus the ranking of each particle in a partial dissolution series of **1** doped with 4.5 mol % of **2**: page 26
Fig. S33. Plot of percentage by HPLC of added impurity in crystals of compound **1** *vs.* the dissolution mid-point for the sample of crystals grown from solutions containing 4.5 mol % of additive **2**: page 27
Fig. S34. Chart comparing particle area versus the ranking of each particle in a partial dissolution series of **1** doped with 5.0 mol % of **2**: page 27
Fig. S35. Chart comparing particle length versus the ranking of each particle in a partial dissolution series of **1** doped with 5.0 mol % of **2**: page 28
Fig. S36. Plot of percentage by HPLC of added impurity in crystals of compound **1** *vs.* the dissolution mid-point for the sample of crystals grown from solutions containing 5.0 mol % of additive **2**: page 28

Table S2. Comparisons of parent batch average and weighted averages from stepwise dissolutions: page 29.

Fig. S37 Comparisons of parent batch average and weighted averages from stepwise dissolutions: page 29.

Table S3. Dissolution mid-points calculated for analysed 4.0 mol % **2**-doped **1** crystals from both observed measurements and 'theoretical' values: page 29.

References: page 30

Synthetic Procedures

Synthesis of 2-nitro-4-*tert*-butylacetanilide (3)

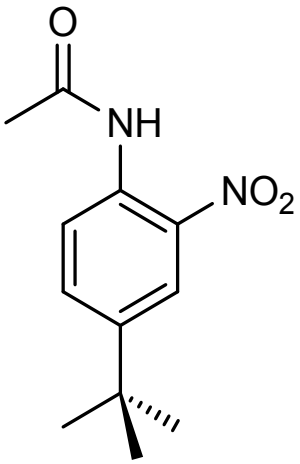

Fig. S1 Chemical structure of 2-Nitro-4-*t*-butylacetanilide **(3)**.

2-Nitro-4-*tert*-butylaniline (3.825 g, 19.693 mmol, 1 eq.), acetic anhydride (3.03 g, 2.8 mL, 29.676 mmol, 1.5 eq.) and two drops of sulphuric acid were stirred together at room temperature to form an orange suspension. The mixture was heated, at approximately 55 °C the mixture solidified but eventually formed an orange coloured solution on continued heating towards 90 °C, at which point it was heated at 90 °C for two hours. After two hours, the reaction was allowed to cool to room temperature and then 30 mL of water was added to precipitate the product. The precipitate was isolated by filtration and washed with two 50 mL portions of water and air dried. The crude product was then recrystallized from 45 mL of hot ethanol, isolated by filtration and washed with two 20 mL portions of ice-cold ethanol. Yield: 2.913 g, 63.14 %. M.P. (DSC) 107.68 °C.

^{1}H NMR (300 MHz, $CDCl_3$): δ 10.18 (s, 1H, NH), 8.63 (d, $^{3}J_{HH}$ = 8.9 Hz, 1H, H-6), 8.17 (d, $^{4}J_{HH}$ = 2.4 Hz, 1H, 3-H), 7.67 (dd, $^{3}J_{HH}$ = 8.9 Hz, $^{4}J_{HH}$ = 2.4 Hz, 1H, 5-H), 2.27 (s, 3H, $H_3CC(O)$), 1.33 (s, 9H, $C(CH_3)_3$).

^{13}C NMR (75 MHz, $CDCl_3$) δ 169.07 (s, C(O)), 147.09 (s, 2-C), 136.40 (s, 4-C), 133.52 (s, 5-C), 132.43 (s, 1-C), 122.26 (s, 6-C), 122.13 (s, 3-C), 34.70 (s, $\underline{C}(CH_3)_3$), 31.09 (s, $C(\underline{C}H_3)_3$), 25.63 (s, $(O)C\underline{C}H_3$).

Elemental analysis: found (calculated) for $C_{12}H_{16}N_2O_3$ (236.12 g mol^{-1}): C, 60.99 (61.00); H, 6.73 (6.83); N, 10.83 (11.86).

NMR Spectra

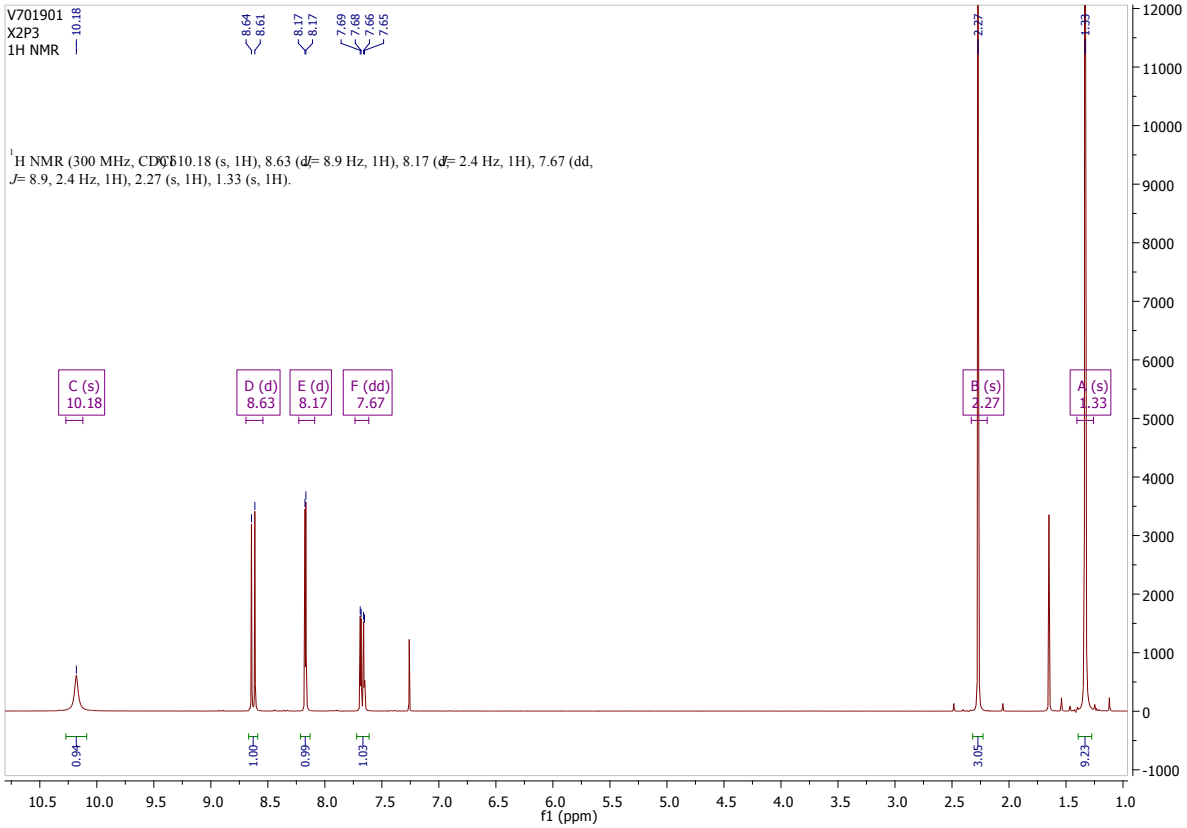

Fig. S2 ^{1}H NMR spectrum of **3** in $CDCl_3$.

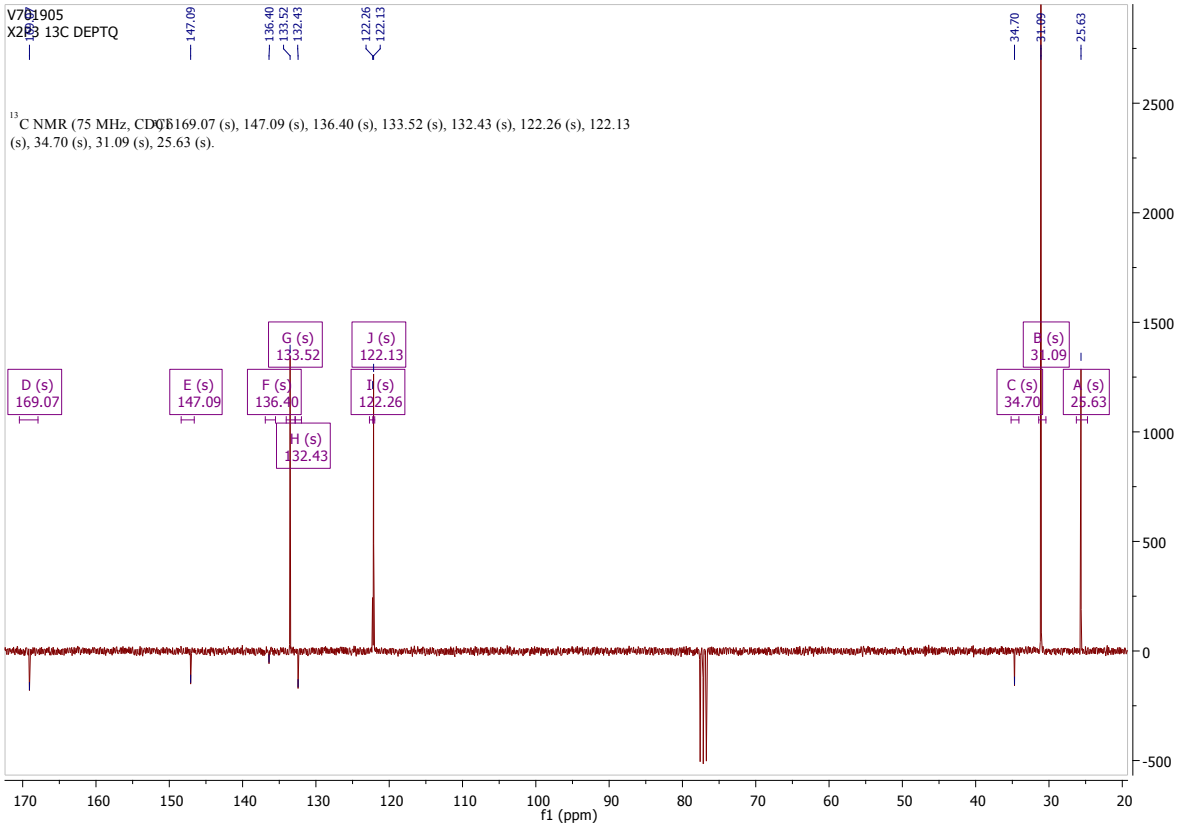

Fig. S3 ^{13}C NMR {^{1}H} (DEPTQ-135) spectrum of **3** in $CDCl_3$.

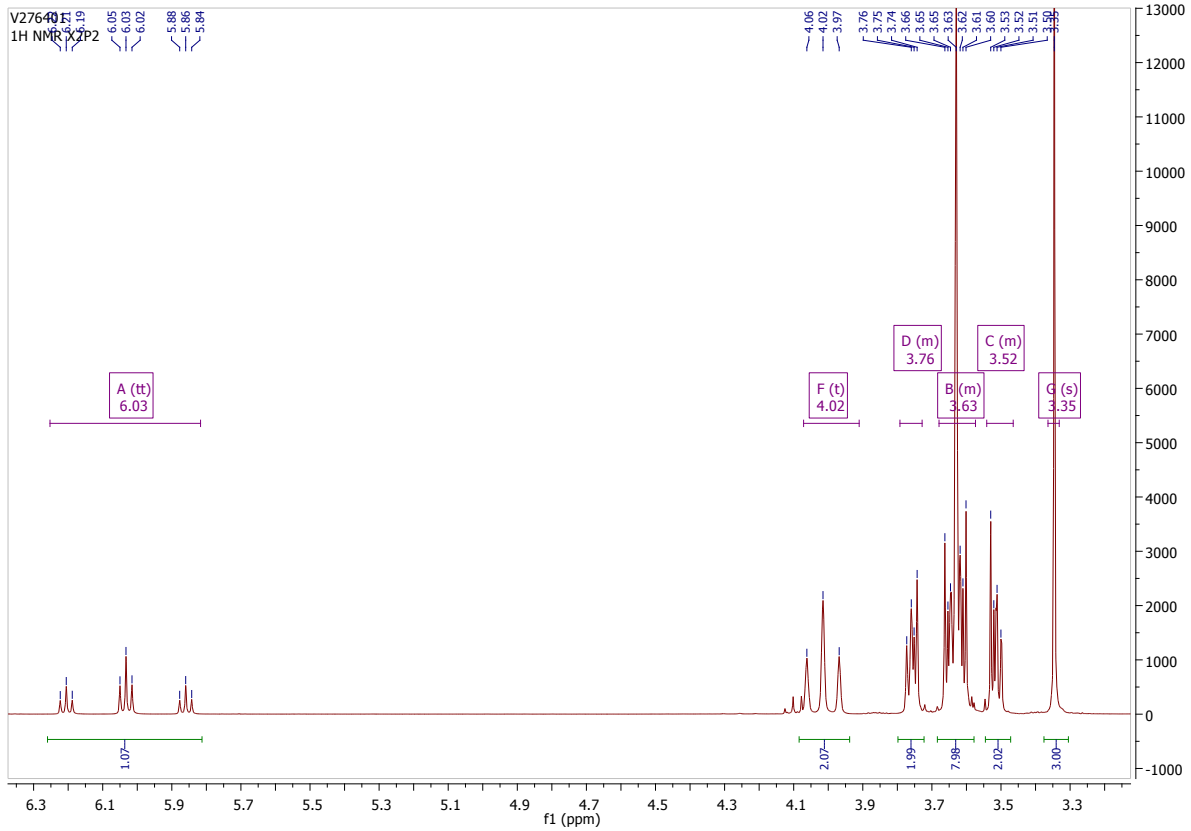

Fig. S4 ^{1}H NMR spectrum of **4** in $CDCl_3$.

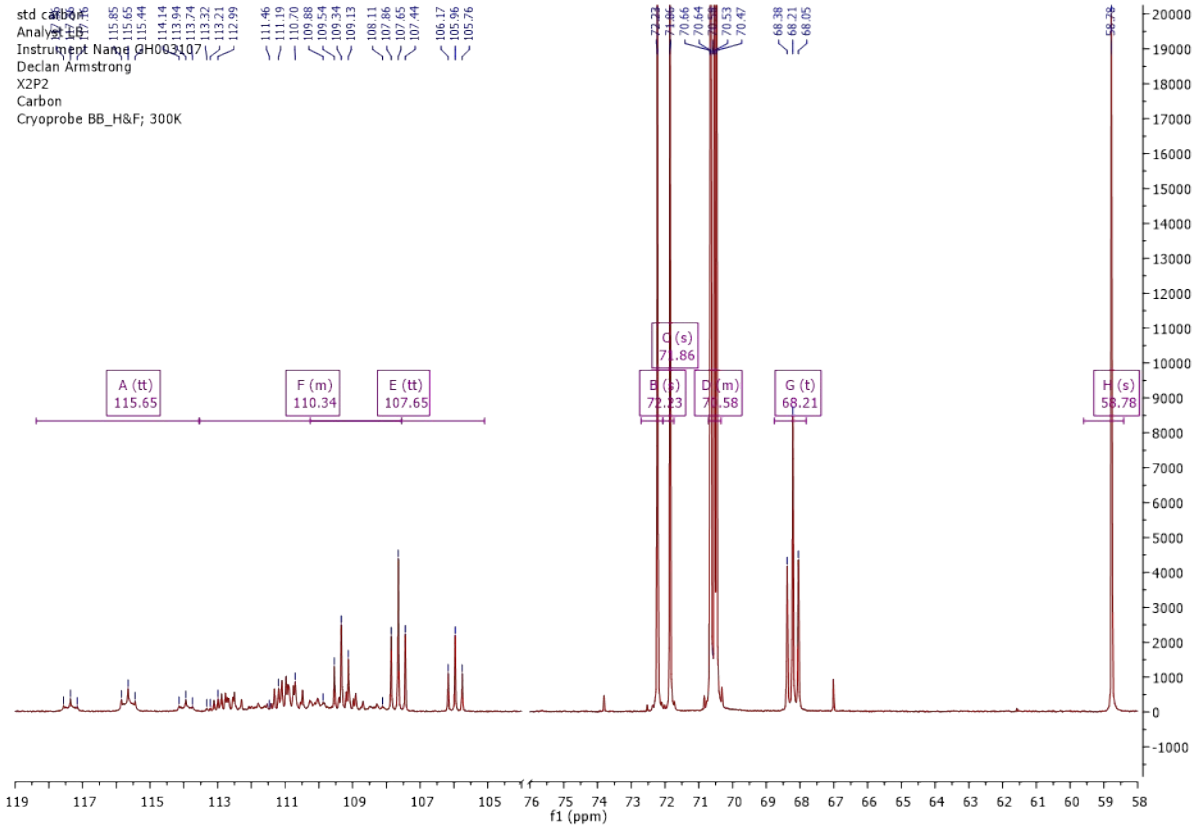

Fig. S5 $^{13}C\{^{1}H\}$ NMR spectrum of **4** in $CDCl_3$.

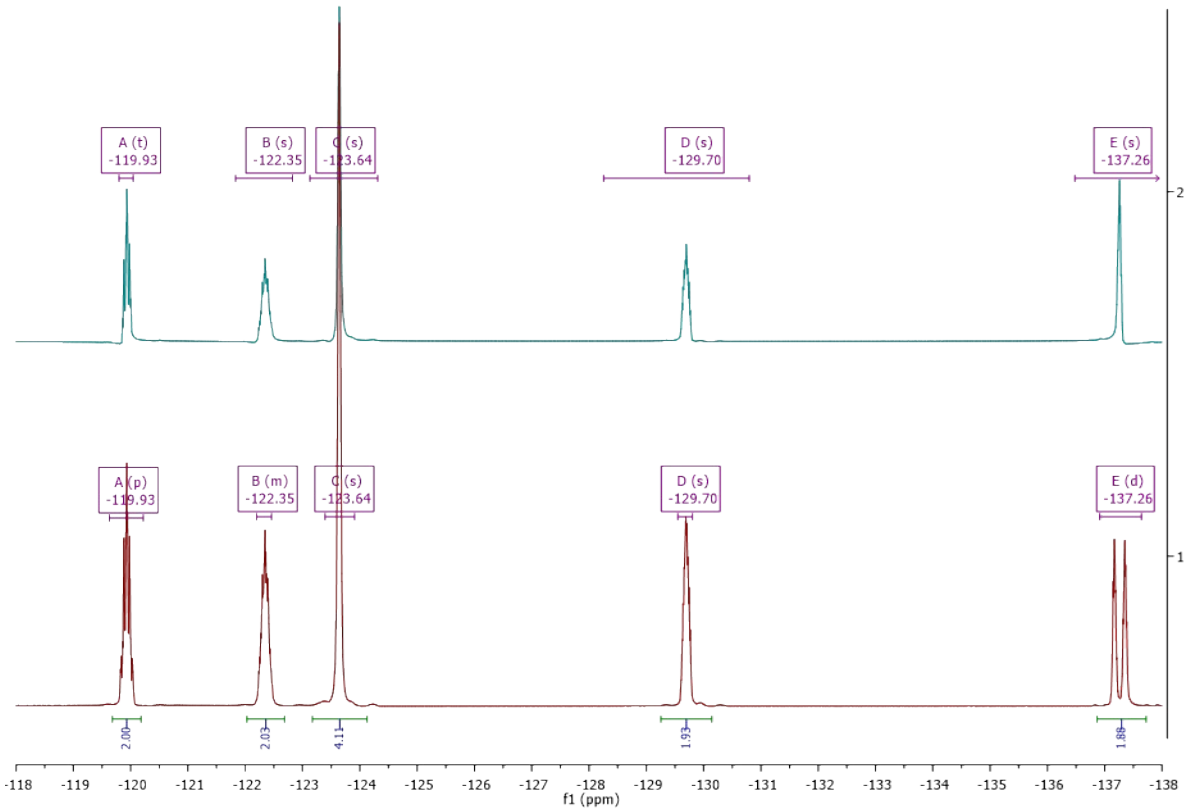

Fig. S6 (Top)(cyan) $^{19}F\{^{1}H\}$ NMR spectrum of **4** in $CDCl_3$. (Bottom)(maroon) ^{19}F NMR spectrum of **4** in $CDCl_3$.

HPLC Calibration Data

HPLC calibration data for method analysing mixtures of compounds **1** and **3**

General Calibration Setting

Calib. Data Modified	Monday, October 01, 2018 9:49:07 AM
Signals calculated separately	No
Rel. Reference Window	5.000 %
Abs. Reference Window	0.000 min
Rel. Non-ref. Window	5.000 %
Abs. Non-ref. Window	0.000 min
Uncalibrated Peaks	not reported
Partial Calibration	Yes, identified peaks are recalibrated
Correct All Ret. Times:	No, only for identified peaks
Curve Type	Linear
Origin	Forced
Weight	Equal
Recalibration Settings:	
Average Response	Average all calibrations
Average Retention Time:	Floating Average New 75%

Signal Details

Signal 1: DAD1 A, Sig=234,4 Ref=360,100

Overview Table

RT	Sig	Lvl	Amount [ng/ul]	Area	Rsp.Factor	Ref	ISTD	#	Compound
1.691	1	1	1.62000	32.07008	5.05144e-2	No	No		**1**
		2	4.05000	76.83419	5.27109e-2				
		3	8.10000	155.67540	5.20313e-2				
		4	16.20000	321.02591	5.04632e-2				
		5	40.50000	808.80182	5.00741e-2				
		6	81.00000	1569.91272	5.15952e-2				
		7	162.00000	3149.05396	5.14440e-2				
		8	405.00000	7813.45020	5.18337e-2				

RT	Sig	Lvl	Amount [ng/ul]	Area	Rsp.Factor	Ref	ISTD	#	Compound
3.664	1	1	1.75000	28.87975	6.05961e-2	No	No		**3**
		2	4.37500	68.86250	6.35324e-2				
		3	8.75000	139.87663	6.25551e-2				
		4	17.50000	289.56149	6.04362e-2				
		5	43.75000	729.74640	5.99523e-2				
		6	87.50000	1419.08252	6.16596e-2				
		7	175.00000	2844.21362	6.15284e-2				
		8	437.50000	7148.04834	6.12055e-2				

==========

Calibration Curves

==========

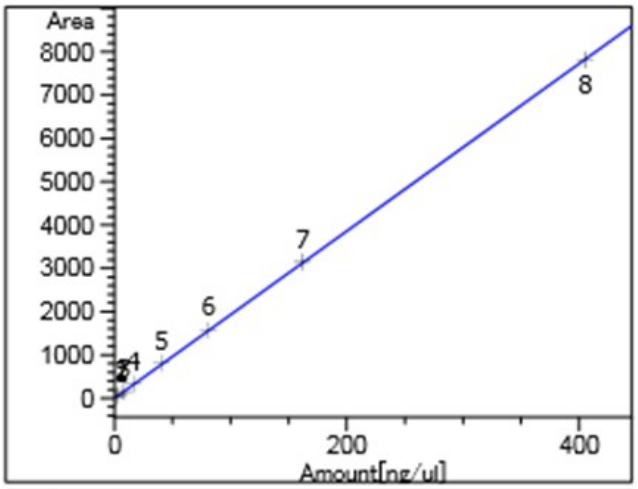

1 at exp. RT: 1.691
DAD1 A, Sig=234,4 Ref=360,100
Correlation: 0.99999
Residual Std. Dev.: 13.52281
Formula: y = mx
m: 19.32094
x: Amount[ng/ul]
y: Area

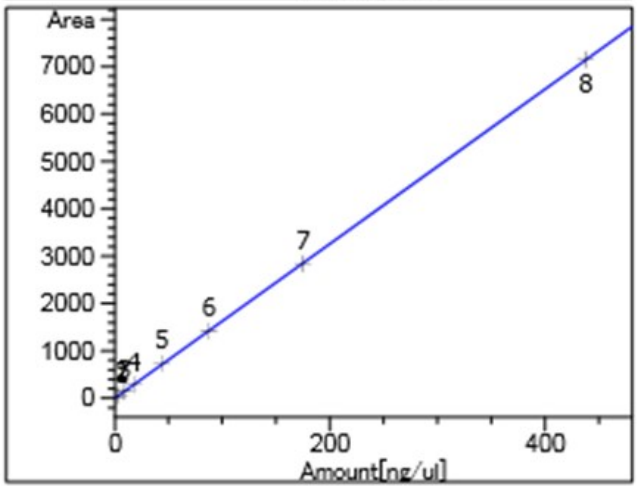

3 at exp. RT: 3.664
DAD1 A, Sig=234,4 Ref=360,100
Correlation: 1.00000
Residual Std. Dev.: 8.89216
Formula: y = mx
m: 16.32604
x: Amount[ng/ul]
y: Area

HPLC calibration data for method analysing mixtures of compounds **1** and **2**

General Calibration Setting

Calib. Data Modified :	Monday, October 01, 2018 10:15:31 AM
Signals calculated separately :	No
Rel. Reference Window :	5.000 %
Abs. Reference Window :	0.000 min
Rel. Non-ref. Window :	5.000 %
Abs. Non-ref. Window :	0.000 min
Uncalibrated Peaks :	not reported
Partial Calibration :	Yes, identified peaks are recalibrated
Correct All Ret. Times:	No, only for identified peaks
Curve Type :	Linear
Origin :	Forced
Weight :	Equal
Recalibration Settings:	
Average Response :	Average all calibrations
Average Retention Time:	Floating Average New 75%

Signal Details

Signal 1: DAD1 A, Sig=234,4 Ref=360,100

Overview Table

RT	Sig	Lvl	Amount [ng/ul]	Area	Rsp.Factor	Ref	ISTD	#	Compound
3.648	1	1	1.33000	30.08573	4.42070e-2	No	No	**2**	
		2	3.32500	74.27542	4.47658e-2				
		3	6.65000	146.36064	4.54357e-2				
		4	13.30000	318.12717	4.18072e-2				
		5	33.25000	776.79382	4.28042e-2				
		6	66.50000	1501.62561	4.42853e-2				
		7	133.00000	2968.40796	4.48052e-2				
		8	332.50000	7522.88916	4.41984e-2				

RT	Sig	Lvl	Amount [ng/ul]	Area	Rsp.Factor	Ref	ISTD	#	Compound
5.121	1	1	1.29000	29.90119	4.31421e-2	No	No	**1**	
		2	3.22500	75.31383	4.28208e-2				
		3	6.45000	148.62427	4.33980e-2				
		4	12.90000	325.70456	3.96064e-2				
		5	32.25000	793.28381	4.06538e-2				
		6	64.50000	1534.63477	4.20295e-2				
		7	129.00000	3038.24951	4.24587e-2				
		8	322.50000	7712.12939	4.18172e-2				

==========

Calibration Curves

==========

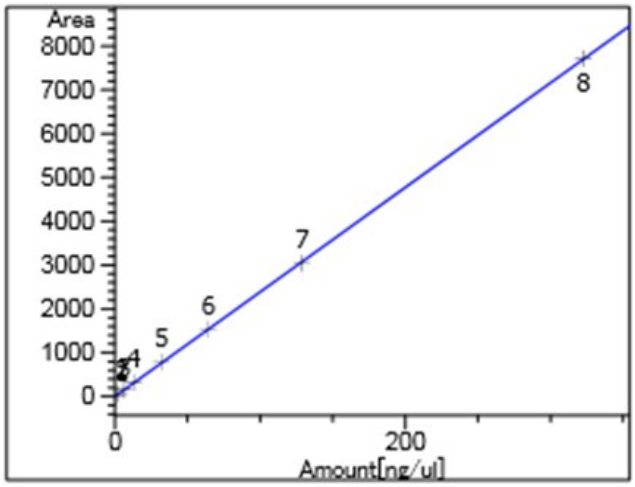

1 at exp. RT: 5.121
DAD1 A, Sig=234,4 Ref=360,100
Correlation: 0.99998
Residual Std. Dev.: 20.00348
Formula: y = mx
m: 23.86897
x: Amount[ng/ul]
y: Area

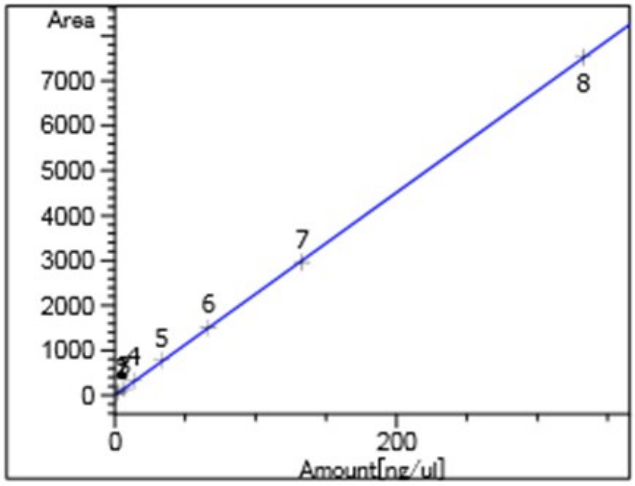

2 at exp. RT: 3.648
DAD1 A, Sig=234,4 Ref=360,100
Correlation: 0.99998
Residual Std. Dev.: 18.61429
Formula: y = mx
m: 22.59089
x: Amount[ng/ul]
y: Area

Particle Sizing

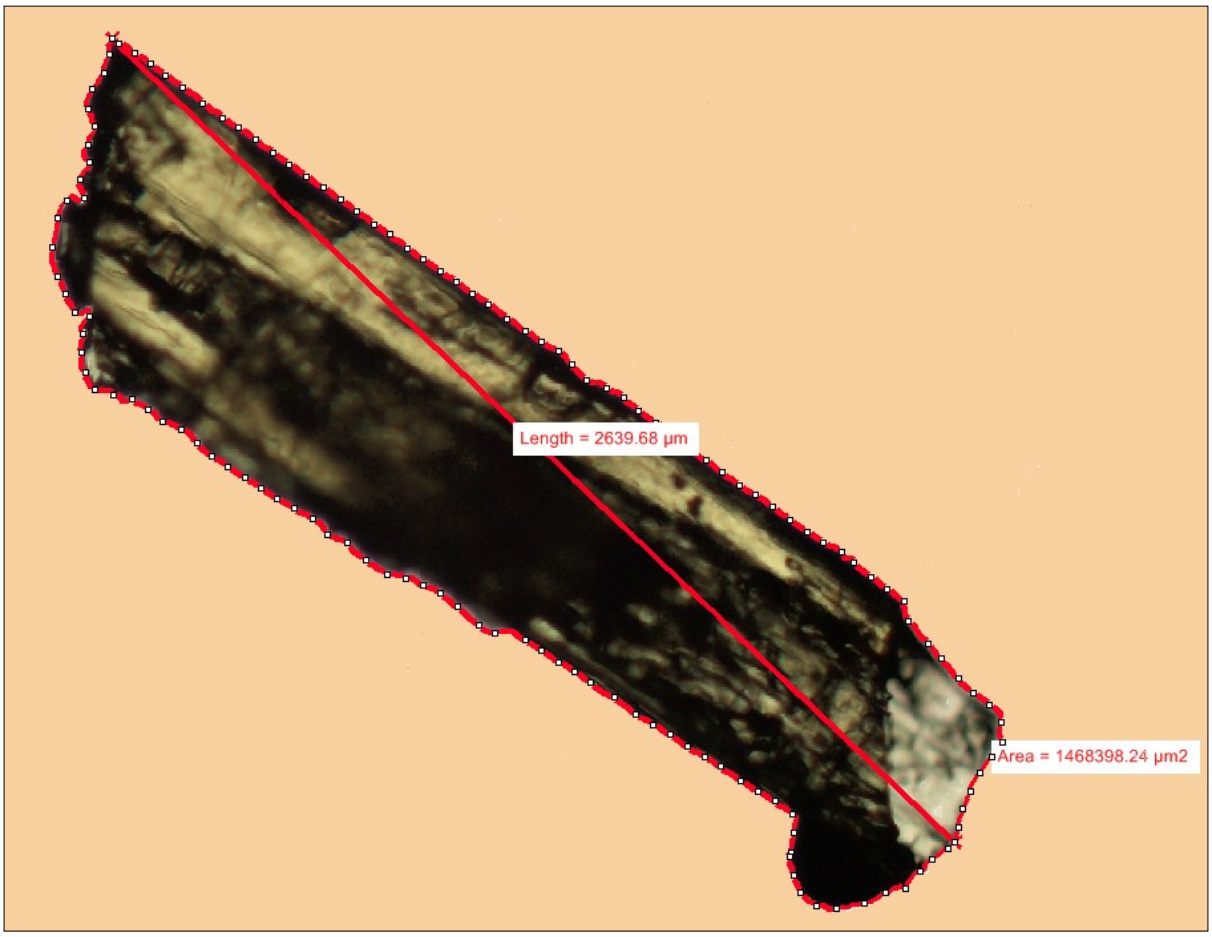

Fig. S7 Image displaying an isolated crystal of compound **1** from a solution doped with 4.0 mol % of compound **2**. This image displays how size measurements were taken; the area in μm^2 was recorded from the area within the external perimeter (highlighted as a red line with white circles); the length in µm was recorded from the longest dimension of the particle (highlighted as a red line bisecting the particle).

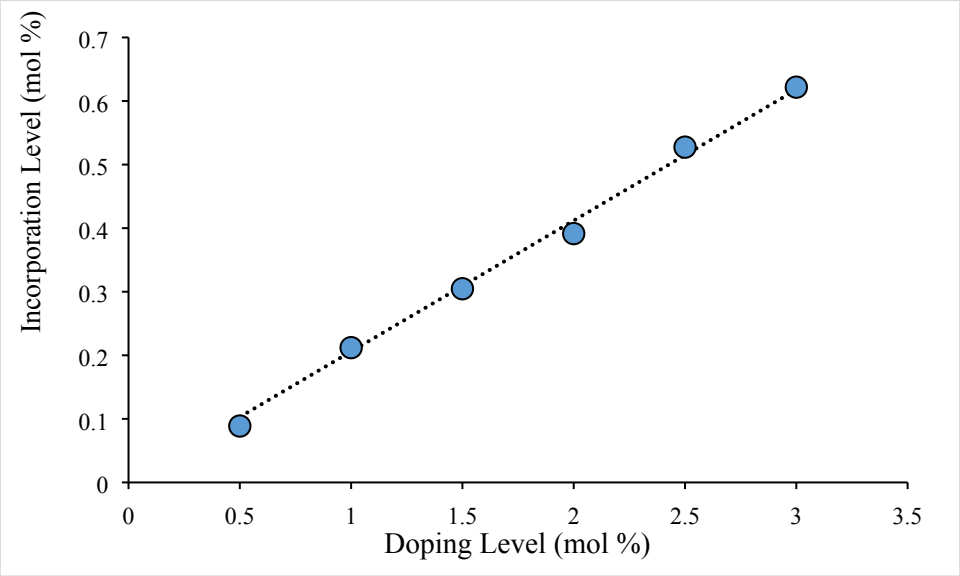

Fig. S8 Graph displaying incorporation level versus solution impurity level of 4-methyl-2-nitroacetanilide (**2**) in "host" 4-trifluoromethyl-2-nitroacetanilide.

Table S1. Overall incorporation (% composition by HPLC) of 4-methyl-2-nitroacetanilide (**2**) and 4-*tert*-butyl-2-nitroacetanilide (**3**) in crystals of 4-chloro-2-nitroacetanilide (**1**) obtained by crystallisation from solutions in toluene containing various quantities of **2** and **3** at a σ value of 1.5. Data is shown for two crystallisation batches.

Level (mol %) of impurity (**2** or **3**) in solution	% **2** incorporated into crystals	% **3** incorporated into first batch of crystals	% **3** incorporated into second batch of crytals
5.0	0.980 (0.03)	0.0992 (0.0002)	0.0599 (0.0002)
4.5	0.917 (0.012)	0.1867 (0.0005)	
4.0	0.838 (0.011)	0.01302 (0.00014)	0.0934 (0.0003)
3.5	0.690 (0.015)	0.0852 (0.0003)	0.0304 (0.0002)
3.0	0.630 (0.05)	0.0564 (0.0002)	0.0717 (0.0004)
2.5	0.497 (0.017)	0.0520 (0.0003)	0.02615 (0.00007)
2.0	0.442 (0.003)	0.0705 (0.0003)	
1.5	0.340 (0.06)	0.0212 (0.0002)	
1.0	0.1980 (0.0014)	0.03897 (0.00009)	
0.5	0.101 (0.003)	0.0172 (0.0003)	

PXRD

Fig. S9 shows the PXRD pattern for **1** grown in toluene at σ = 1.5 against the PXRD patterns for **1** grown in toluene at σ = 1.5 with 5 mol % additions **2**. The PXRD pattern for **2** grown under the same conditions is also added for reference. PXRD patterns were obtained for crystals of **1** with additive concentrations as low as 0.5% grown under the aforementioned conditions, however, for none of the samples, as can be seen at the highest additive concentration of **2**, there is no discernible formation of additional diffraction peaks. All obtained patterns displayed peaks corresponding to that of **1** with only minor differences in the intensities of some of the peaks peaks.

A similar image comparing the PXRD patterns based around compound **3** can be seen in Fig. S10. This figure compares the PXRD patterns for crystals related to pure **1**, 4.5 mol % **3**-doped **1**, and pure **3**, all grown in toluene at σ = 1.5. Again, the sample doped with impurity displays no diffraction peaks other than from the pure **1** sample with minor differences in intensity.

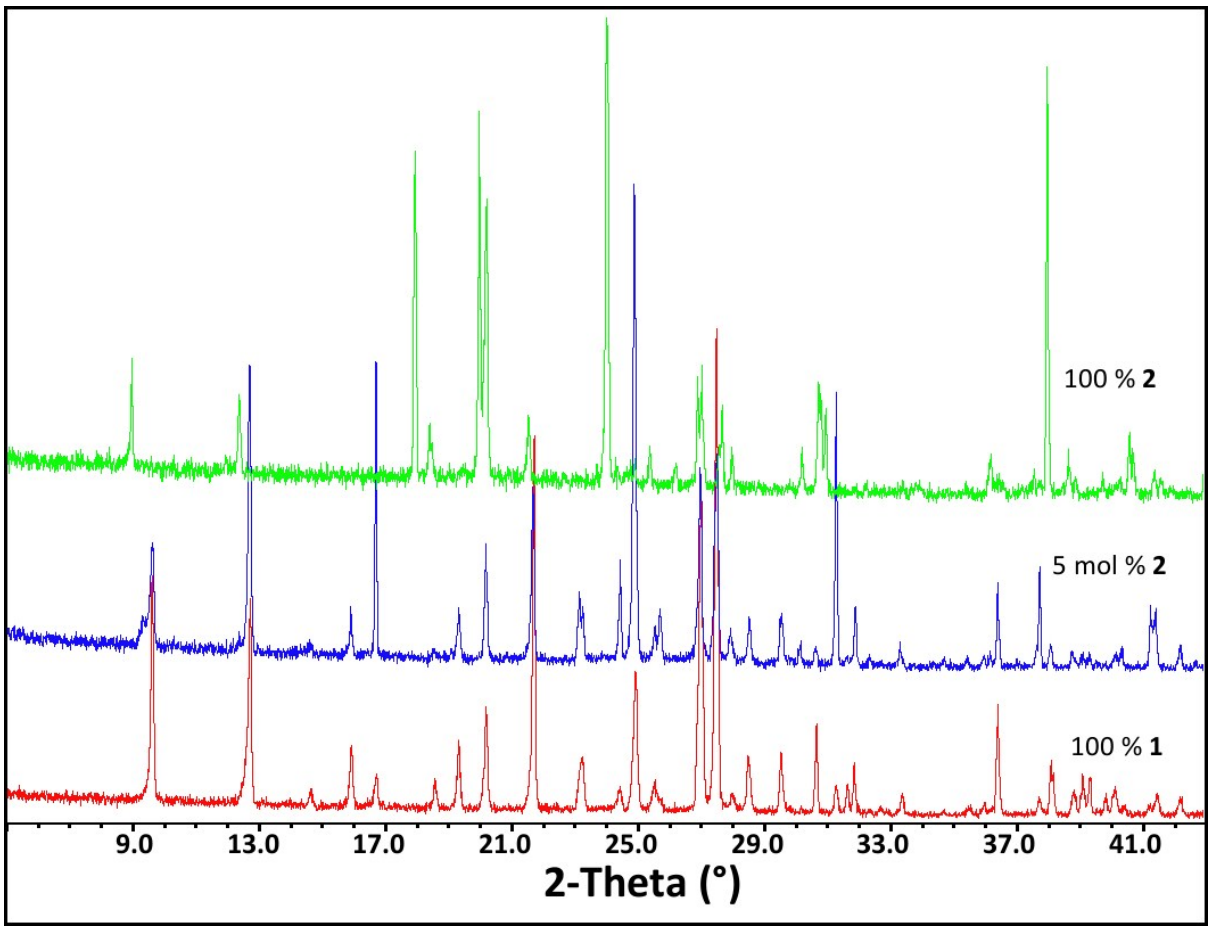

Fig. S9 Powder X-ray diffraction patterns obtained for crystals of **1** grown from toluene (red), **1** grown from toluene with concentrations of 5 mol% **2** (blue), and **2** grown from toluene (green).

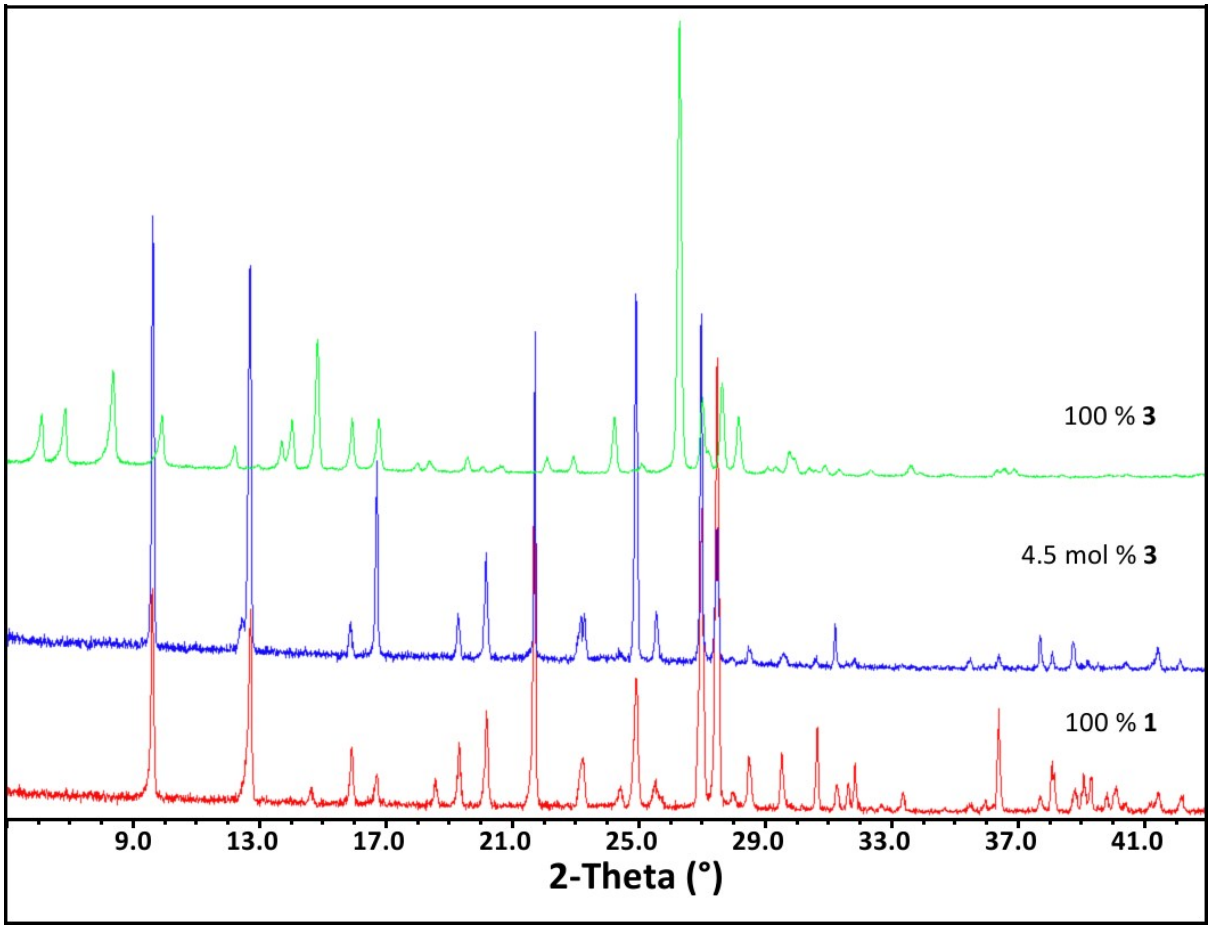

Fig. S10 Powder X-ray diffraction patterns obtained for crystals of **1** grown from toluene (red), **1** grown from toluene with concentrations of 4.5 mol % **3** (blue), and **3** grown from toluene (green).

Differential Scanning Calorimetry

The DSC curves for pure compounds **1** and **2**, and 5 mol % **2**-doped **1** are displayed in Fig. S11. The inclusion of additive at the highest level in this study did not alter the melting point of the crystals in any significant way, as the melting of 99.51 °C is for the impurity-doped sample is marginally higher than the melting point of 99.44 °C for pure compound **1**.

Fig. S12 shows the DSC curves for pure compounds **1** and **3**, and 4.5 mol % **3**-doped **1**. Again the impurity-doped sample shows a minimal difference in melting point, rising to 100.11 °C from 99.44 °C for pure compound **1**.

None of the samples displayed in Fig. S11 and Fig. S12 showed any secondary events such as minor melting points or polymorph changes under the tested conditions.

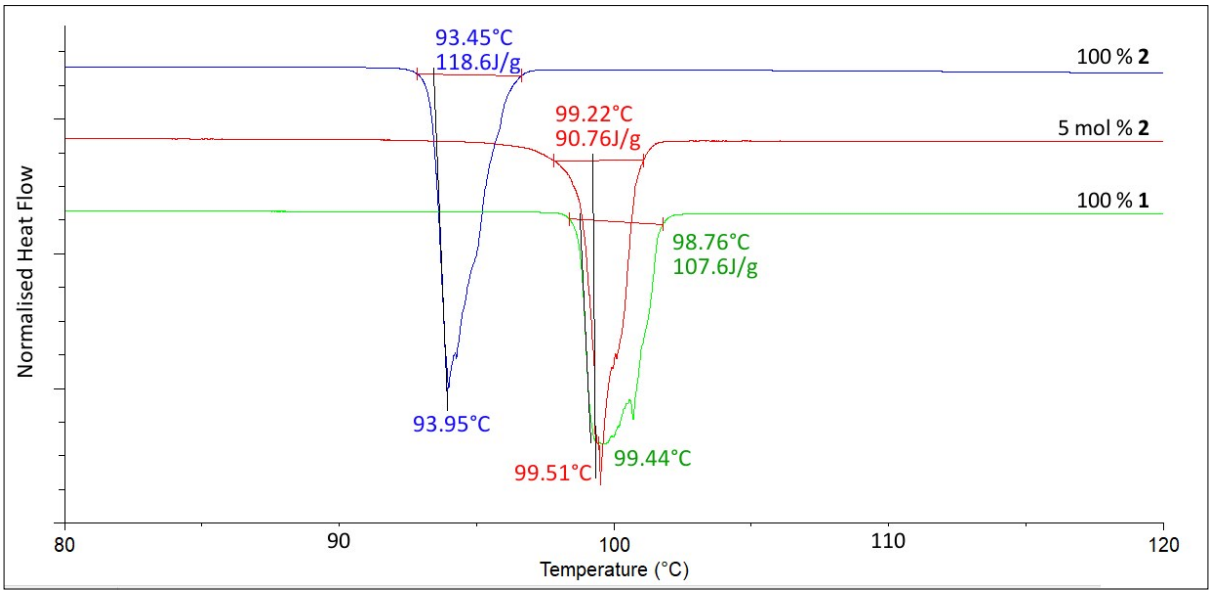

Fig. S11 DSC curves obtained from crystals of **1** containing 5 mol % **2** (red); compared to DSC curves of component compounds **1** (green) and **2** (blue).

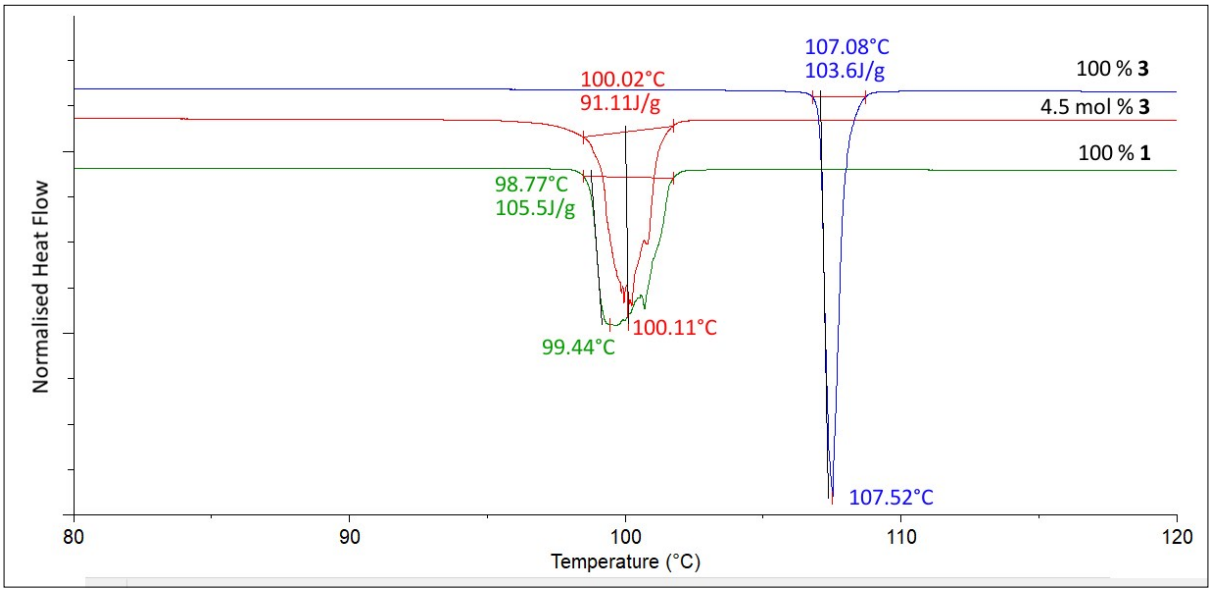

Fig. S12 DSC curves obtained from crystals of **1** containing 4.5 mol % **3** (red); compared to DSC curves of component compounds **1** (green) and **3** (blue).

Partial Dissolution Graphs

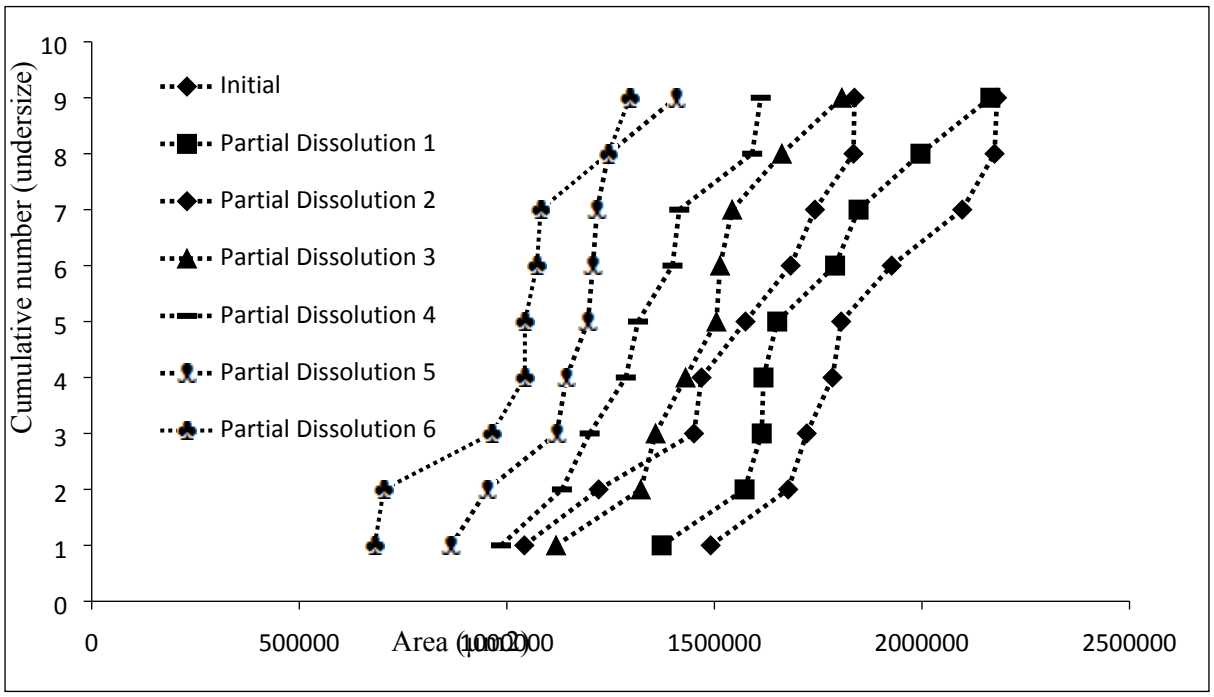

Fig. S13 Chart comparing particle area versus the ranking of each particle in a partial dissolution series of **1** doped with 1.5 mol % of **2**.

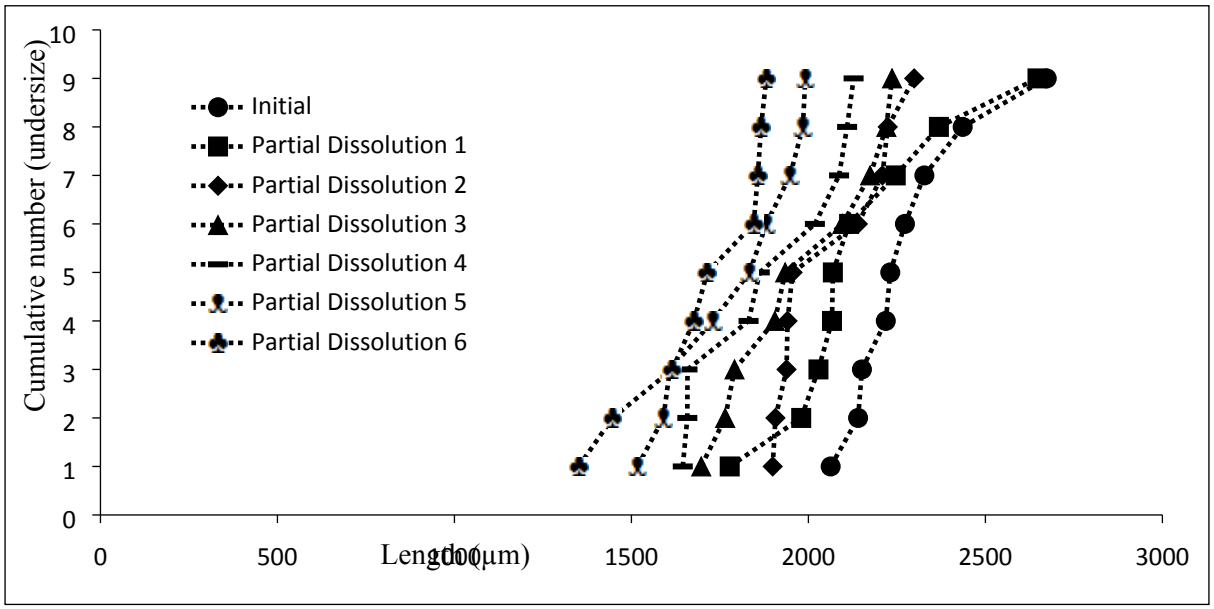

Fig. S14 Chart comparing particle length versus the ranking of each particle in a partial dissolution series of **1** doped with 1.5 mol % of **2**.

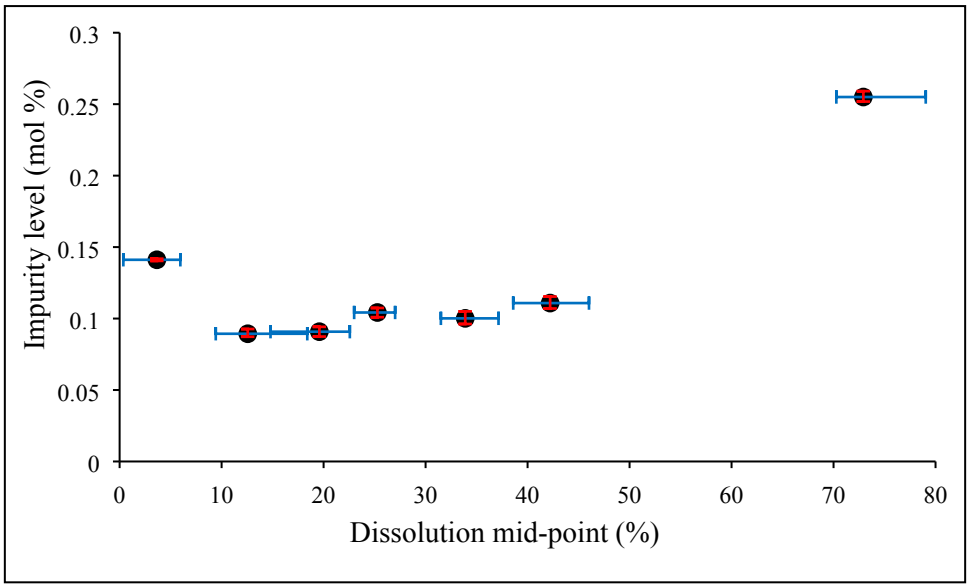

Fig. S15 Plot of percentage by HPLC of added impurity in crystals of compound **1** *vs.* the dissolution mid-point for the sample of crystals grown from solutions containing 1.5 mol % of additive **2**.

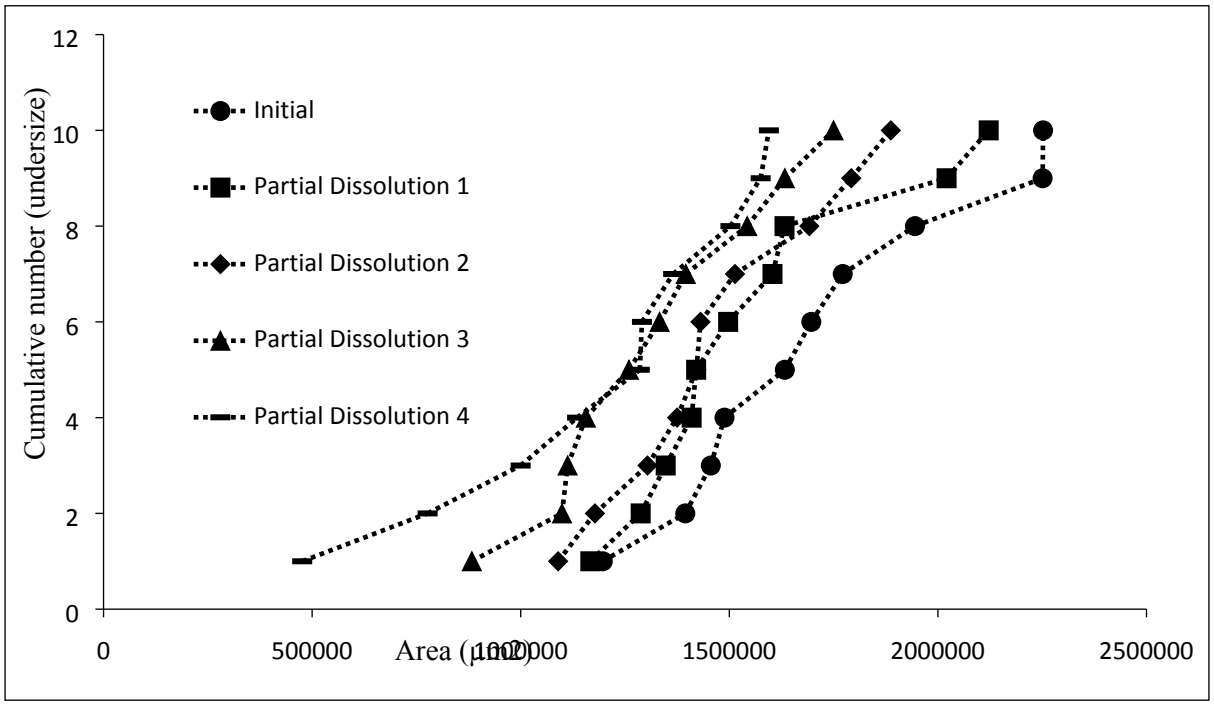

Fig. S16 Chart comparing particle area versus the ranking of each particle in a partial dissolution series of **1** doped with 2.0 mol % of **2**.

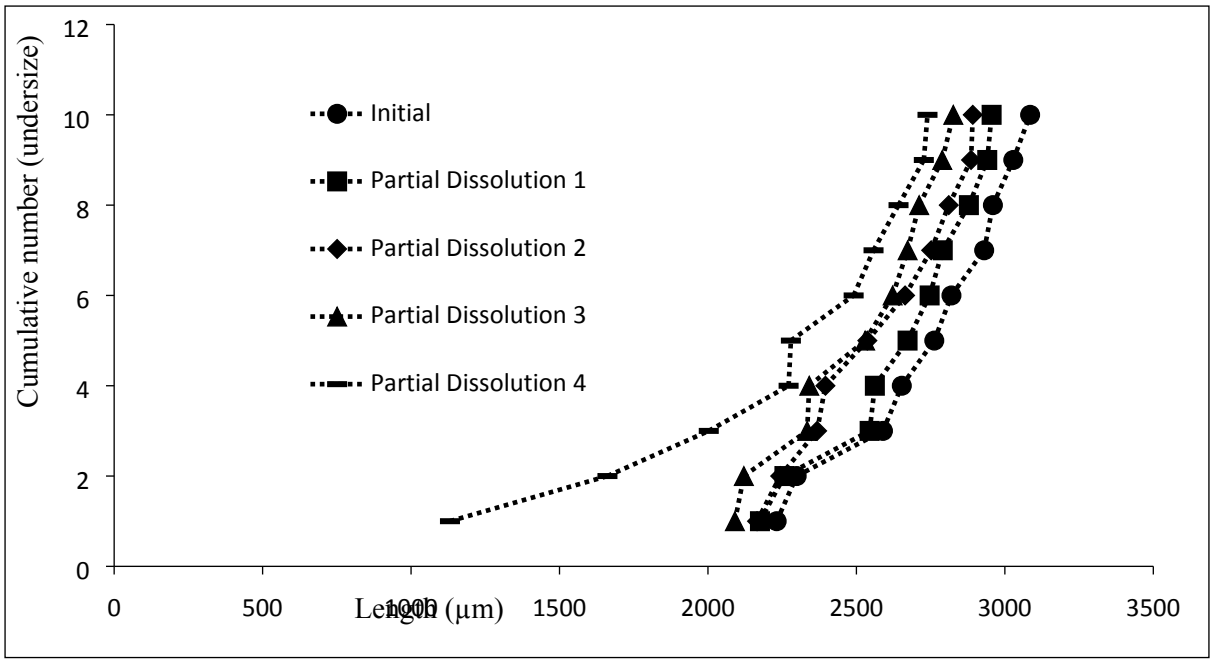

Fig. S17 Chart comparing particle length versus the ranking of each particle in a partial dissolution series of **1** doped with 2.0 mol % of **2**.

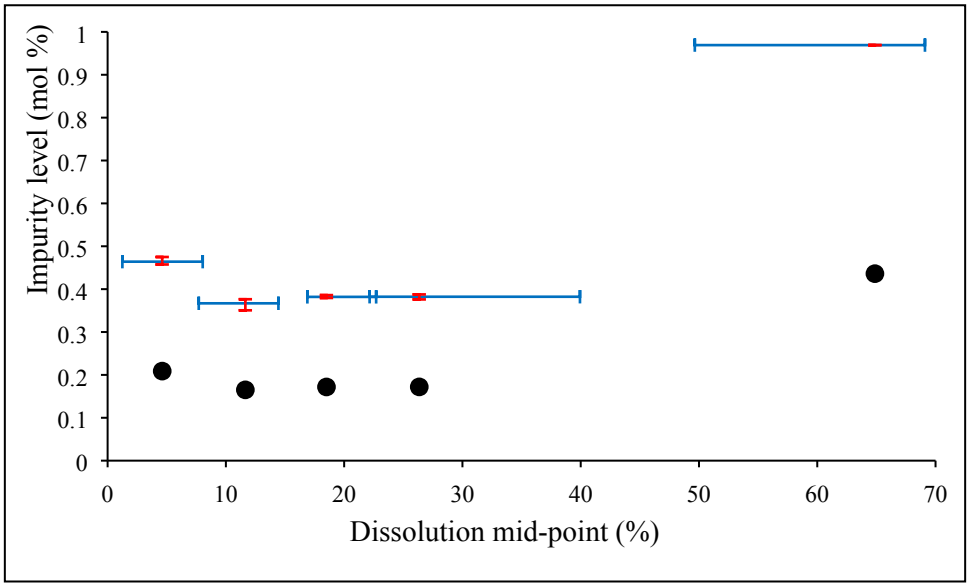

Fig. S18 Plot of percentage by HPLC of added impurity in crystals of compound **1** *vs.* the dissolution mid-point for the sample of crystals grown from solutions containing 2.0 mol % of additive **2**.

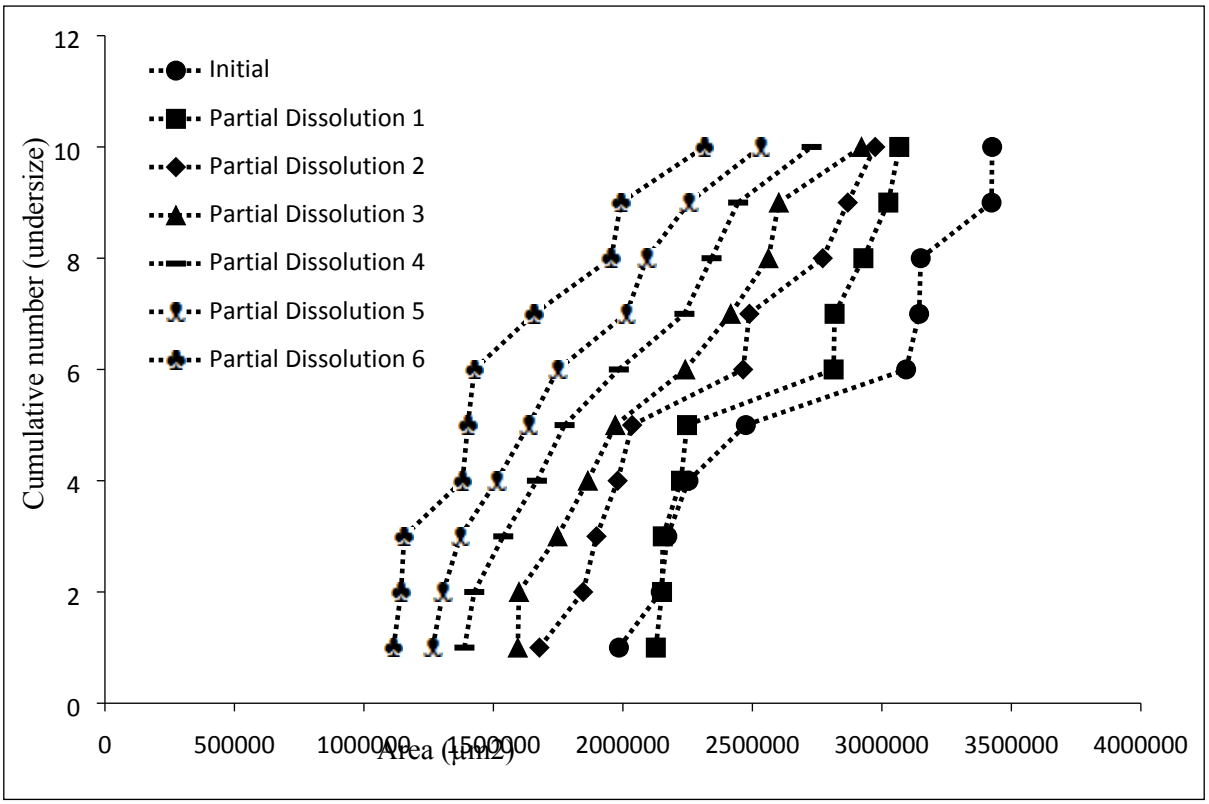

Fig. S19 Chart comparing particle area versus the ranking of each particle in a partial dissolution series of **1** doped with 2.5 mol % of **2**.

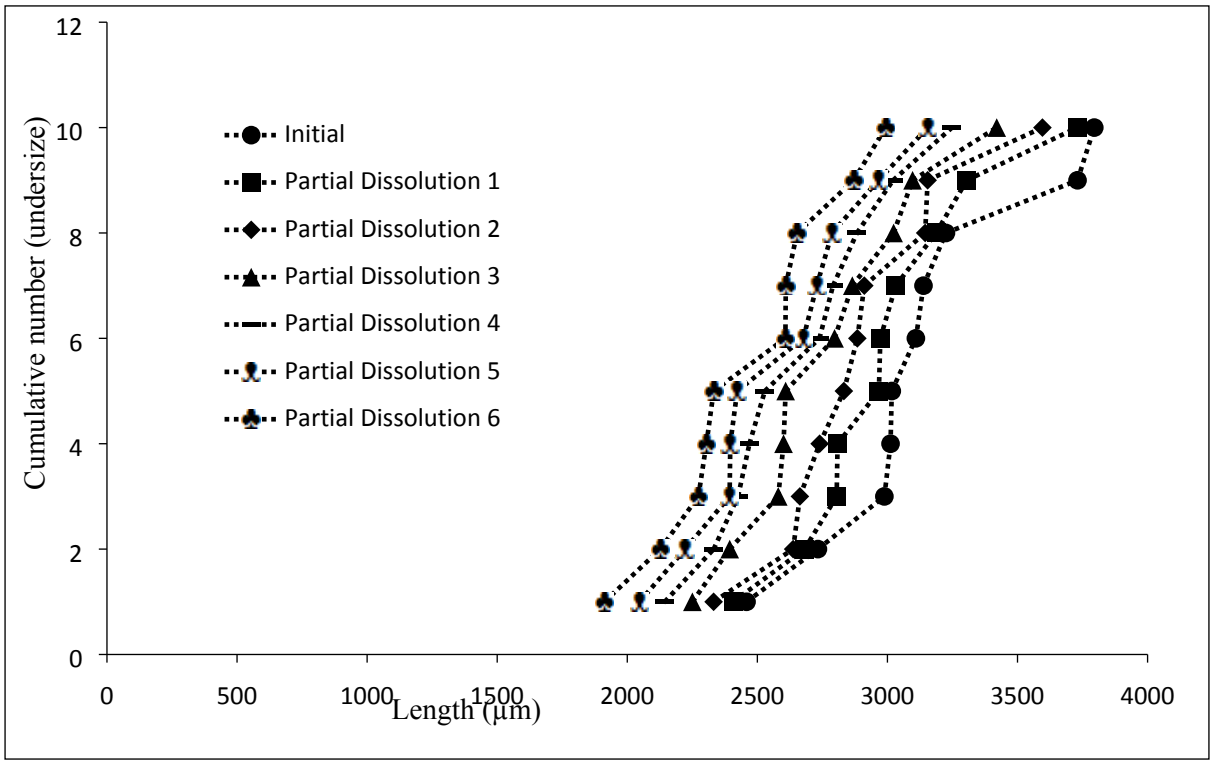

Fig. S20 Chart comparing particle length versus the ranking of each particle in a partial dissolution series of **1** doped with 2.5 mol % of **2**.

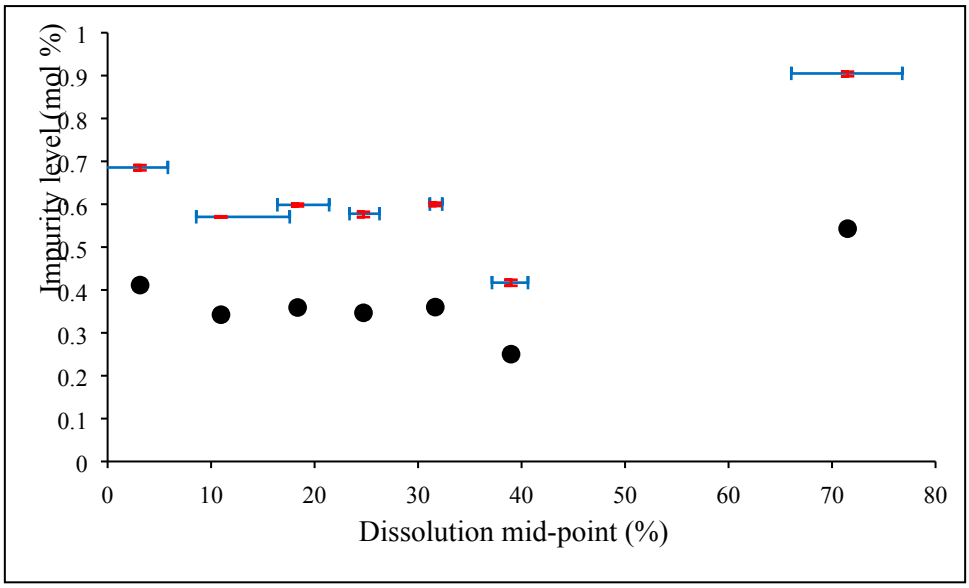

Fig. S21 Plot of percentage by HPLC of added impurity in crystals of compound **1** *vs.* the dissolution mid-point for the sample of crystals grown from solutions containing 2.5 mol % of additive **2**.

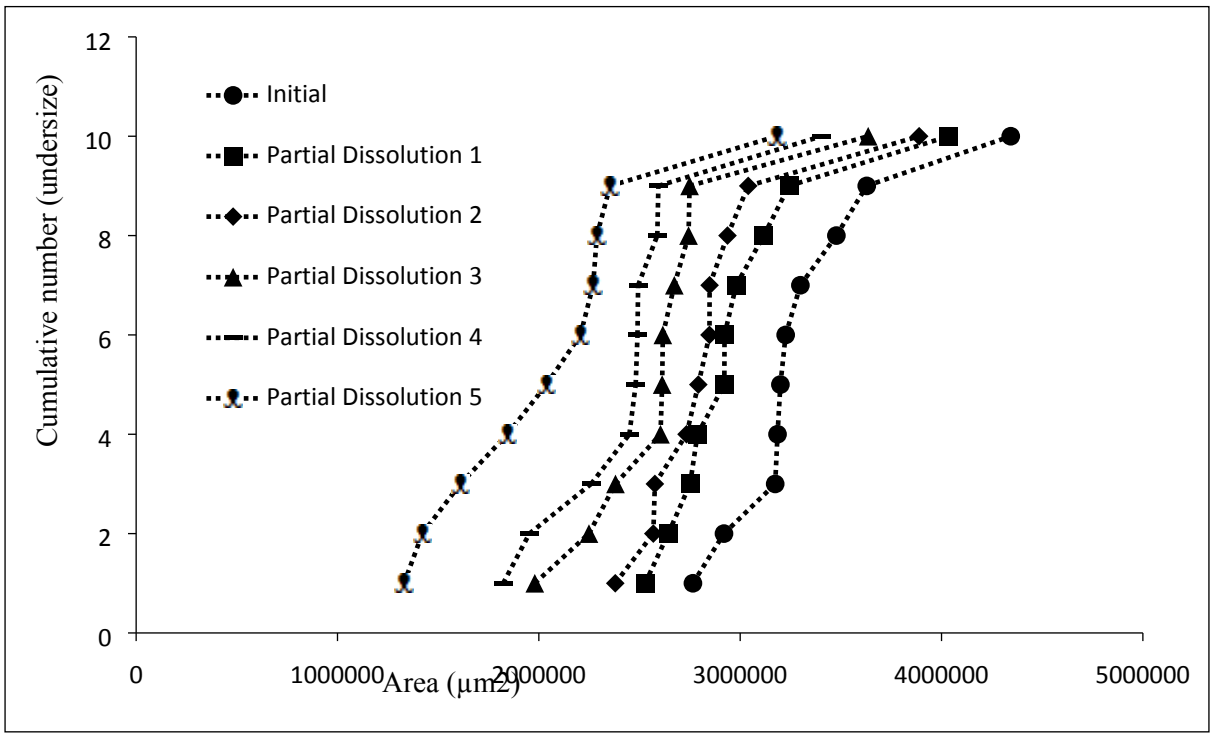

Fig. S22 Chart comparing particle area versus the ranking of each particle in a partial dissolution series of **1** doped with 3.0 mol % of **2**.

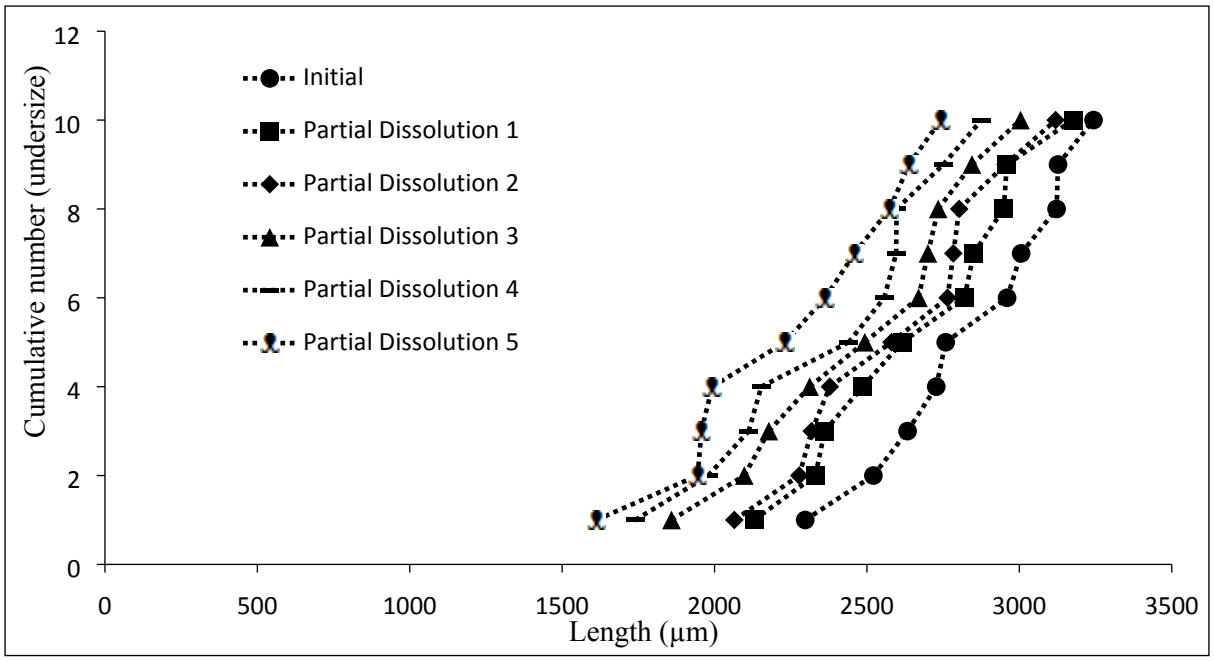

Fig. S23 Chart comparing particle length versus the ranking of each particle in a partial dissolution series of **1** doped with 3.0 mol % of **2**.

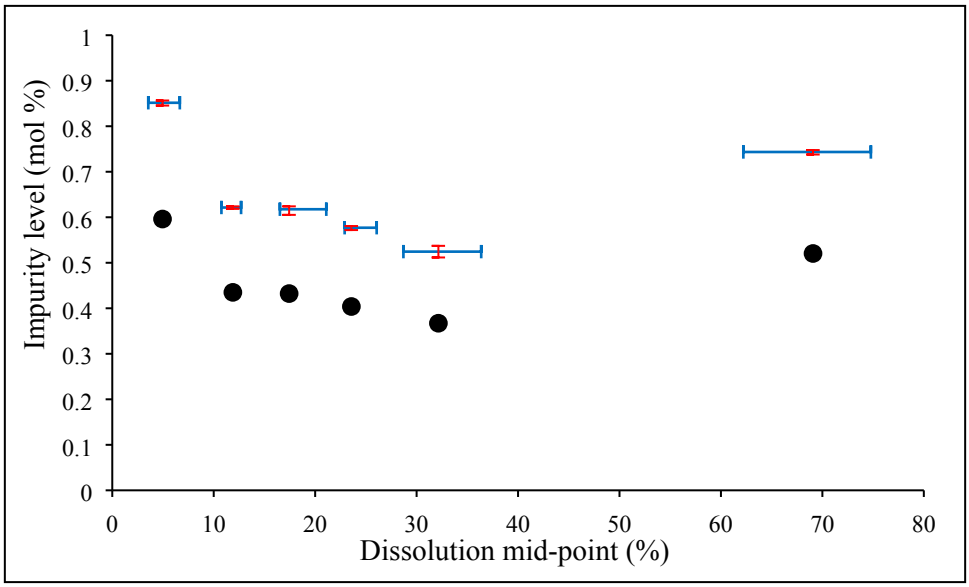

Fig. S24 Plot of percentage by HPLC of added impurity in crystals of compound **1** *vs.* the dissolution mid-point for the sample of crystals grown from solutions containing 3.0 mol % of additive **2**.

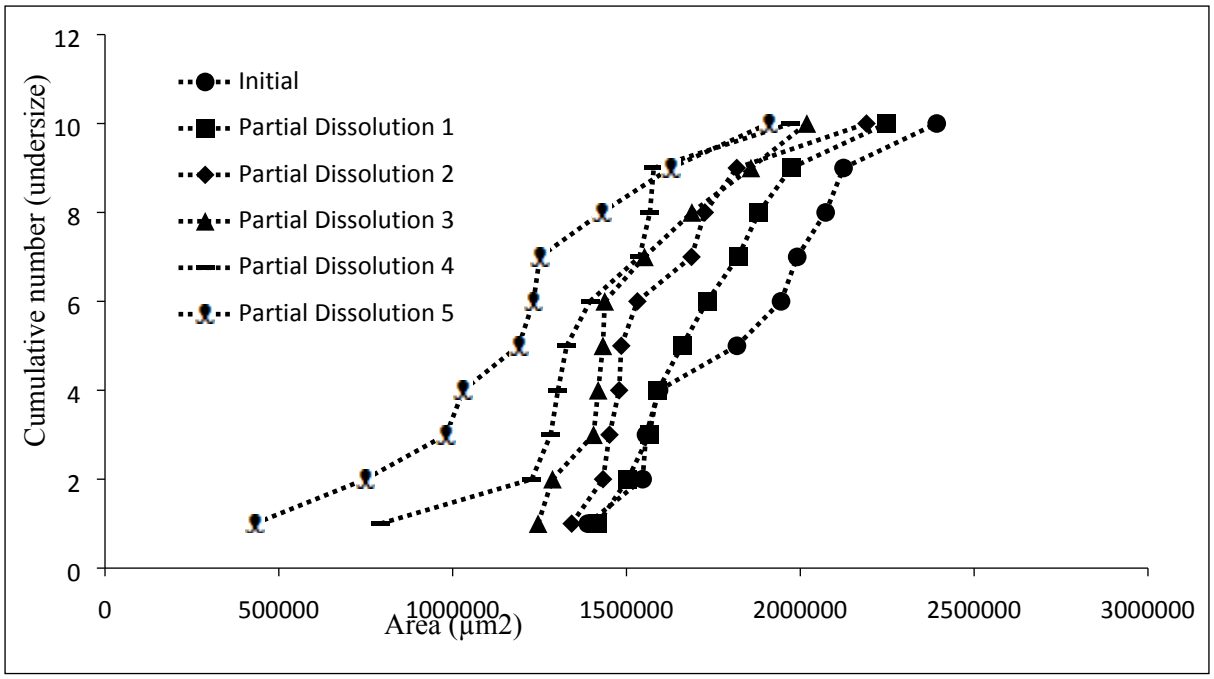

Fig. S25 Chart comparing particle area versus the ranking of each particle in a partial dissolution series of **1** doped with 3.5 mol % of **2**.

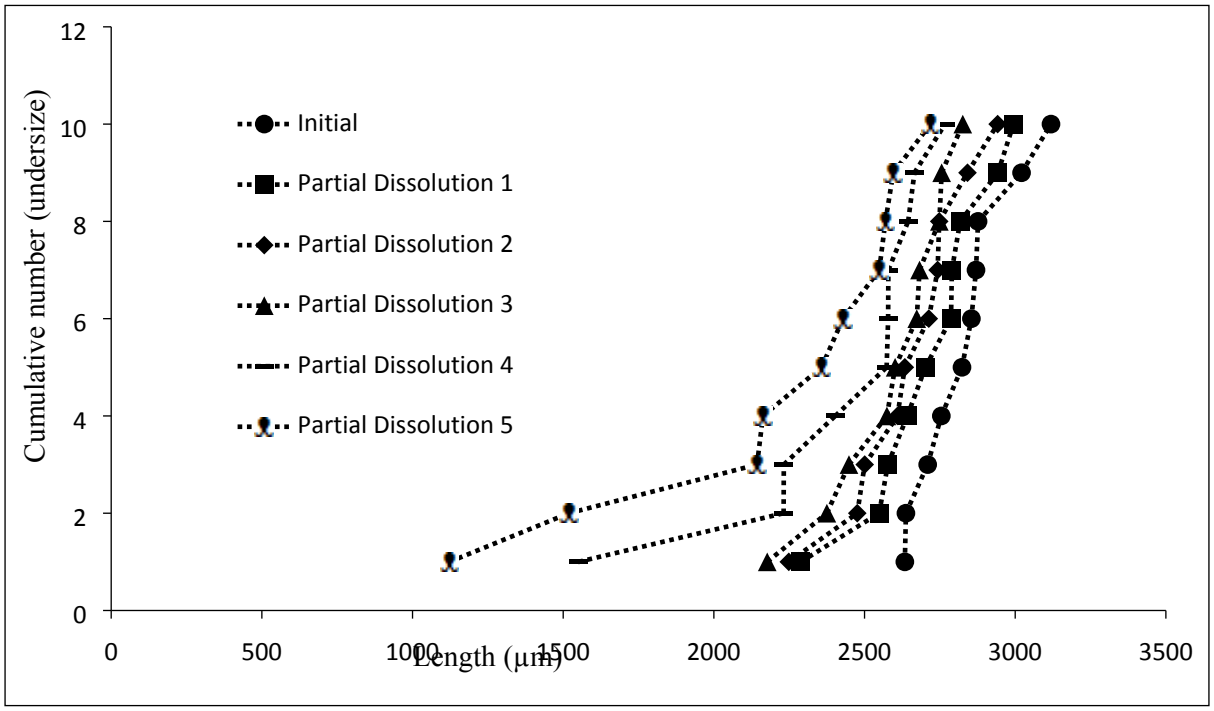

Fig. S26 Chart comparing particle length versus the ranking of each particle in a partial dissolution series of **1** doped with 3.5 mol % of **2**.

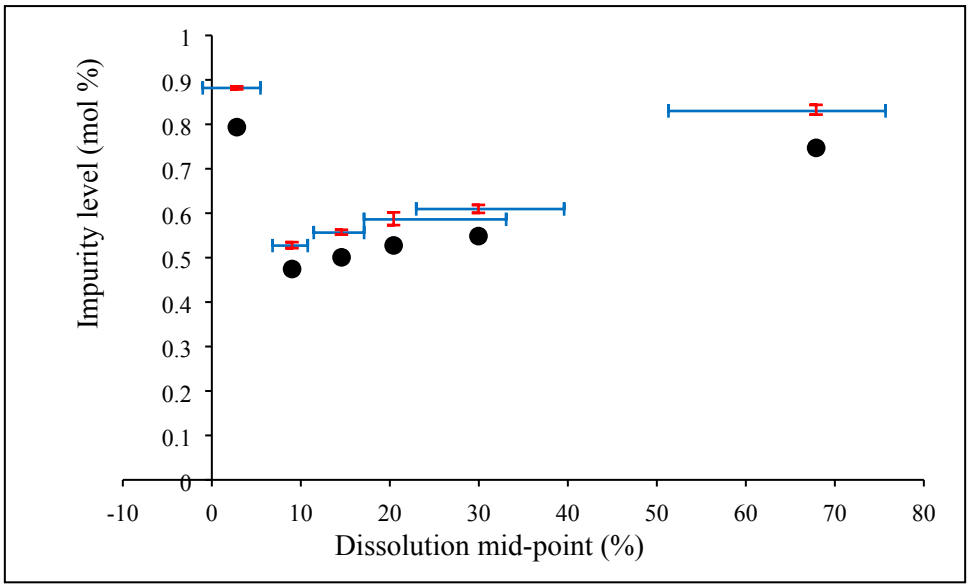

Fig. S27 Plot of percentage by HPLC of added impurity in crystals of compound **1** *vs.* the dissolution mid-point for the sample of crystals grown from solutions containing 3.5 mol % of additive **2**.

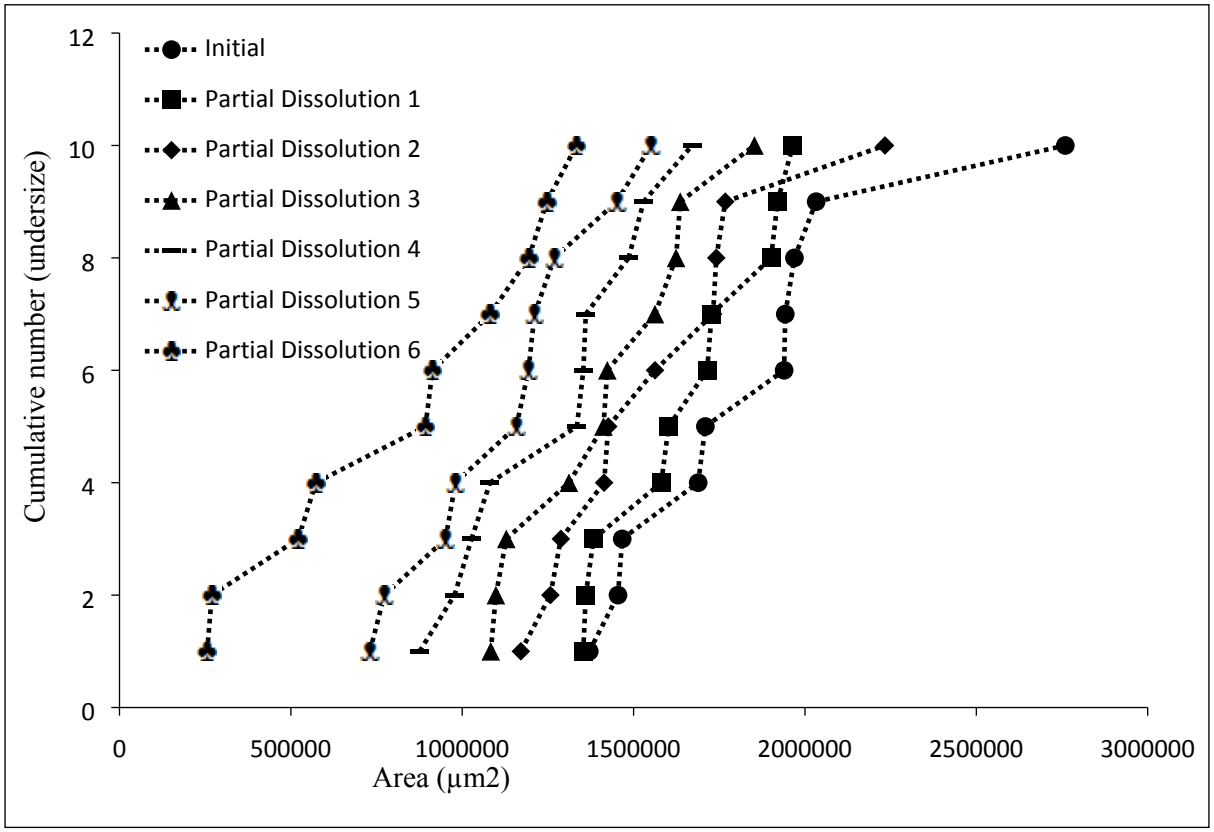

Fig. S28 Chart comparing particle area versus the ranking of each particle in a partial dissolution series of **1** doped with 4.0 mol % of **2**.

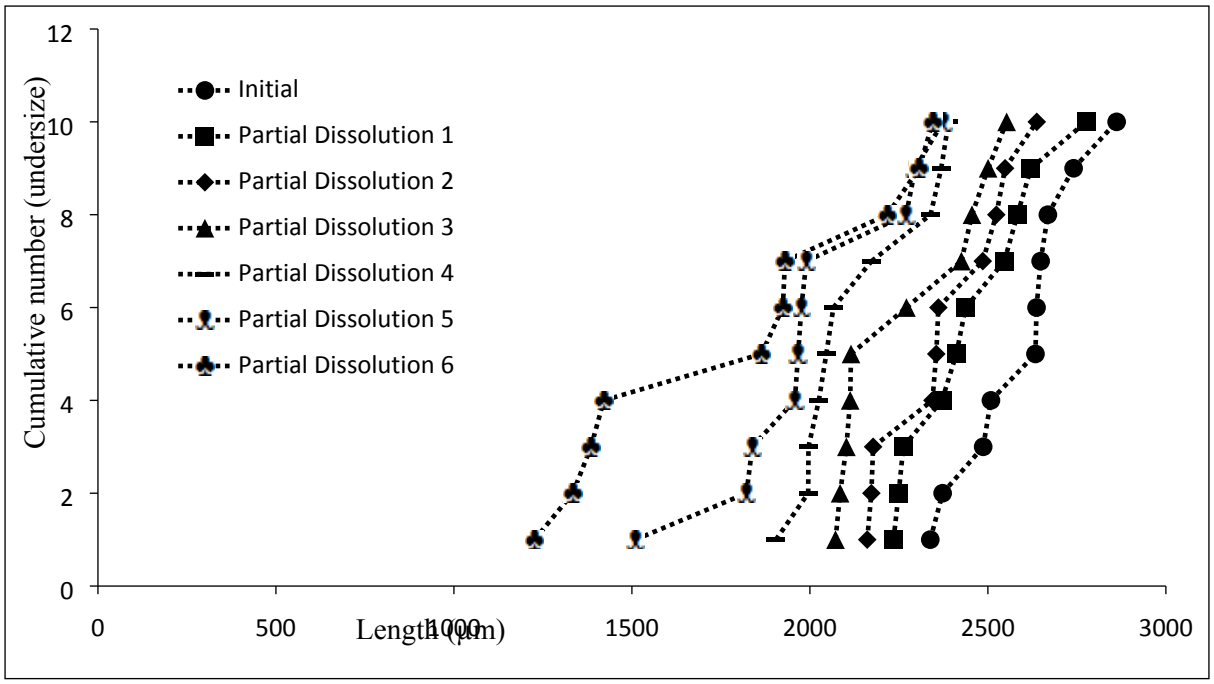

Fig. S29 Chart comparing particle length versus the ranking of each particle in a partial dissolution series of **1** doped with 4.0 mol % of **2**.

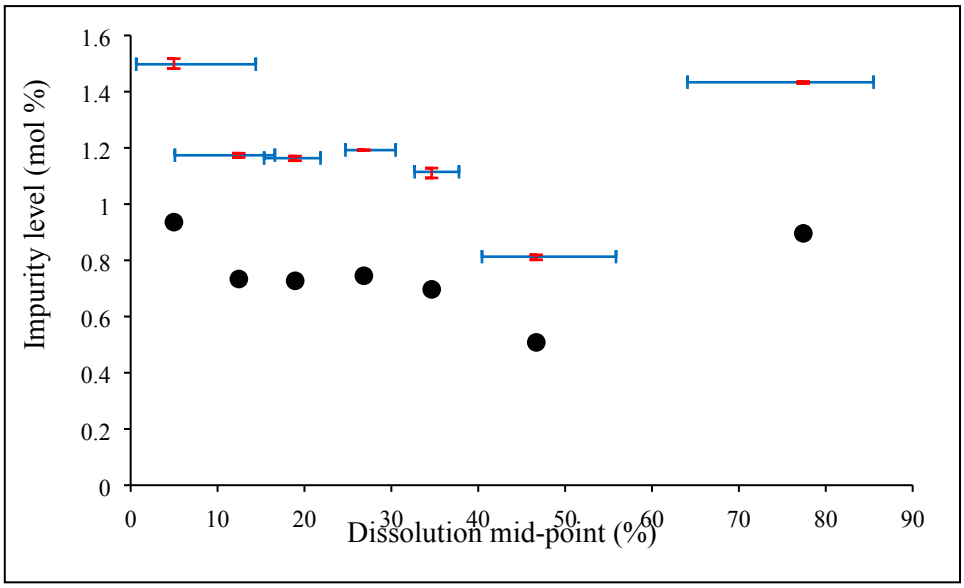

Fig. S30 Plot of percentage by HPLC of added impurity in crystals of compound **1** *vs.* the dissolution mid-point for the sample of crystals grown from solutions containing 4.0 mol % of additive **2**.

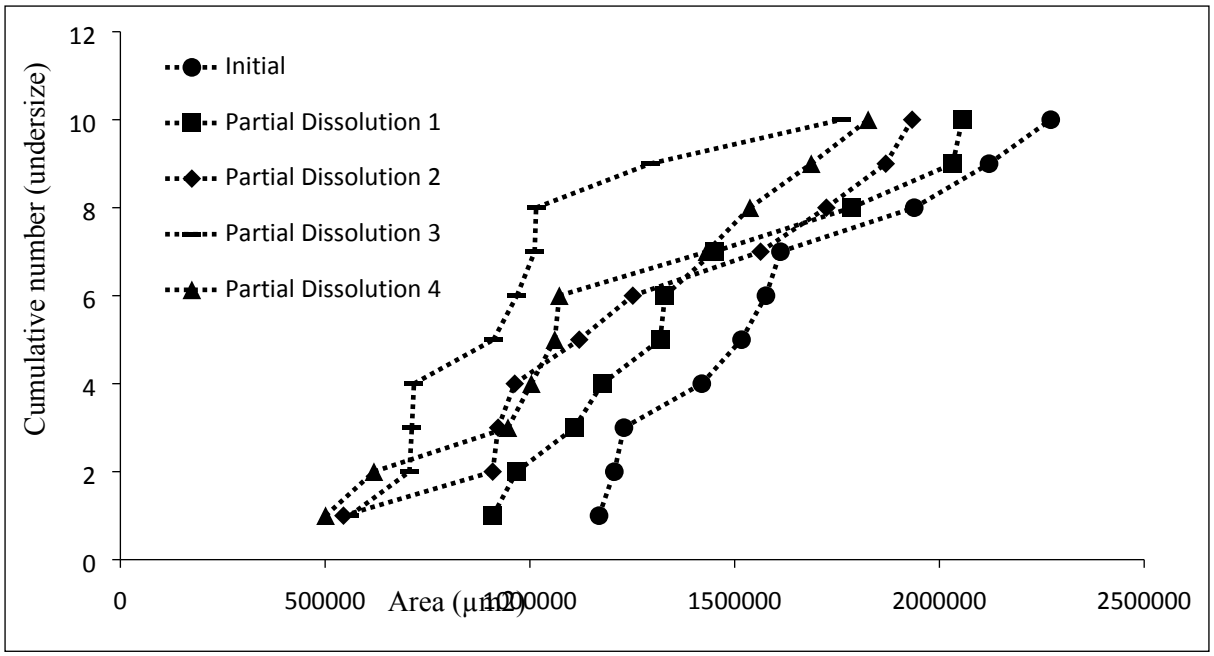

Fig. S31 Chart comparing particle area versus the ranking of each particle in a partial dissolution series of **1** doped with 4.5 mol % of **2**.

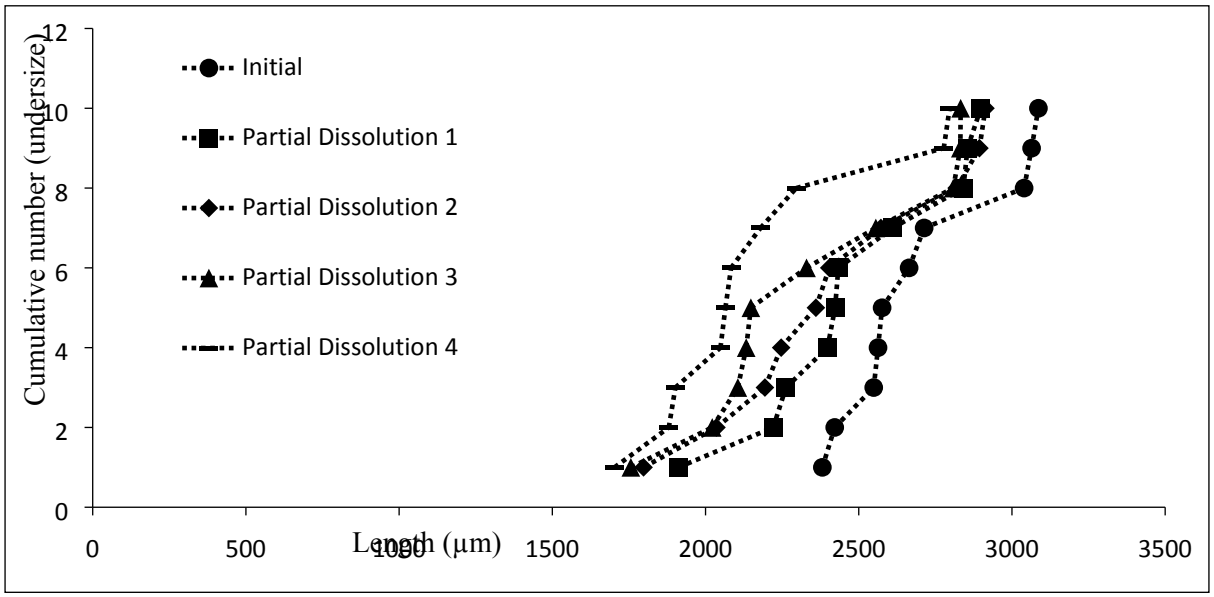

Fig. S32 Chart comparing particle length versus the ranking of each particle in a partial dissolution series of **1** doped with 4.5 mol % of **2**.

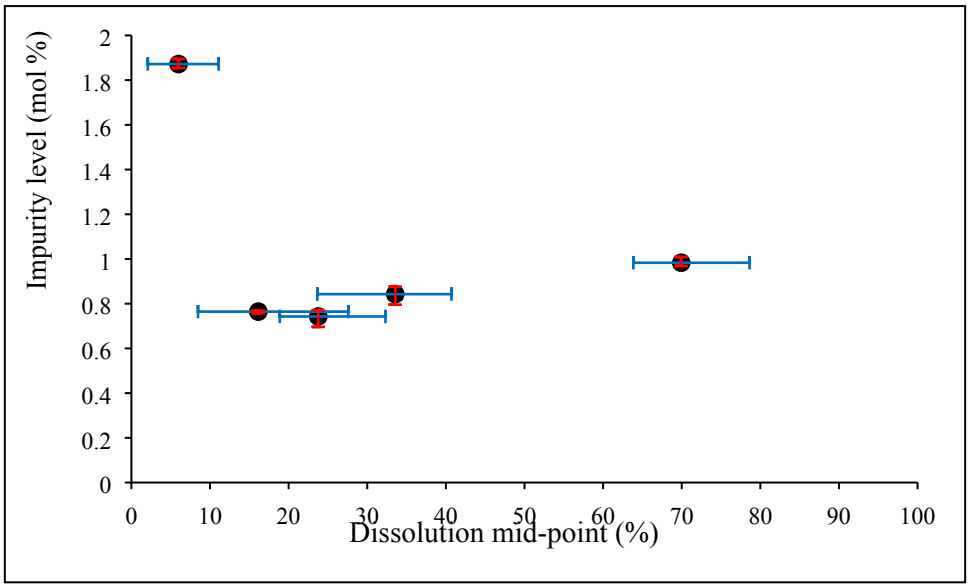

Fig. S33 Plot of percentage by HPLC of added impurity in crystals of compound **1** *vs.* the dissolution mid-point for the sample of crystals grown from solutions containing 4.5 mol % of additive **2**.

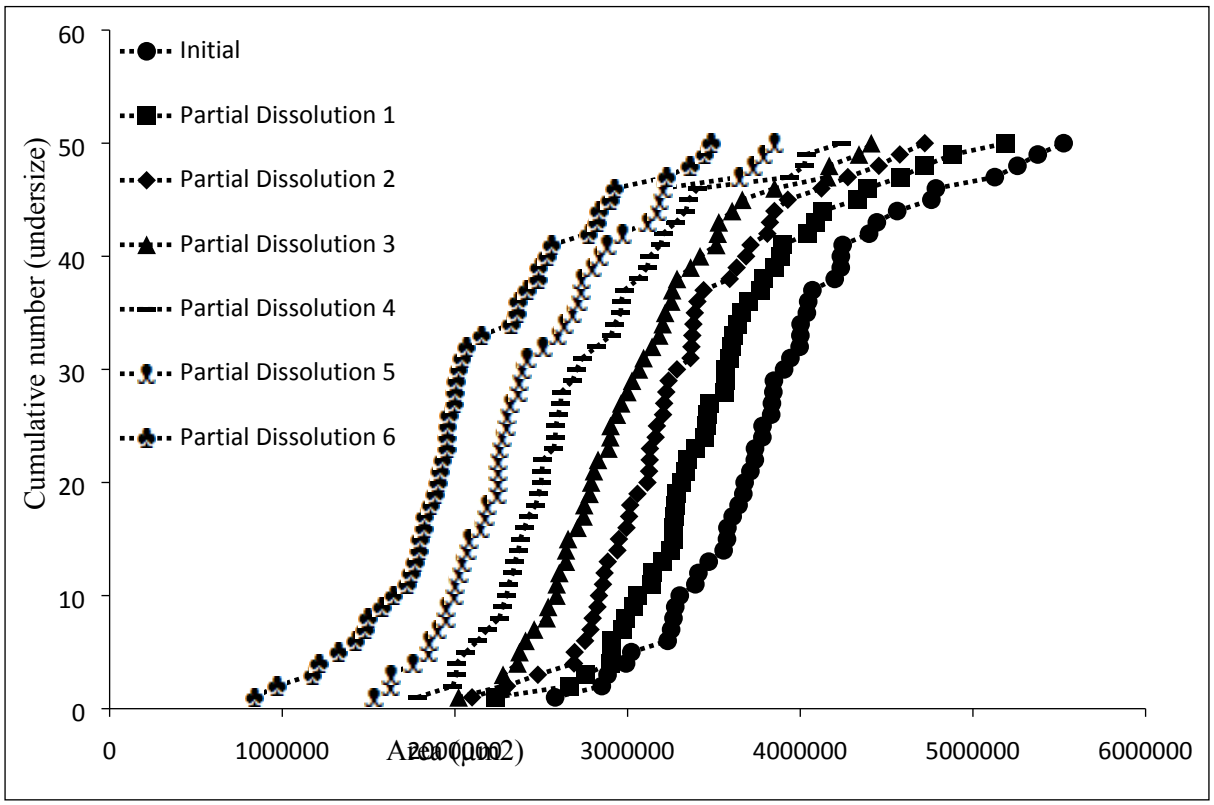

Fig. S34 Chart comparing particle area versus the ranking of each particle in a partial dissolution series of **1** doped with 5.0 mol % of **2**.

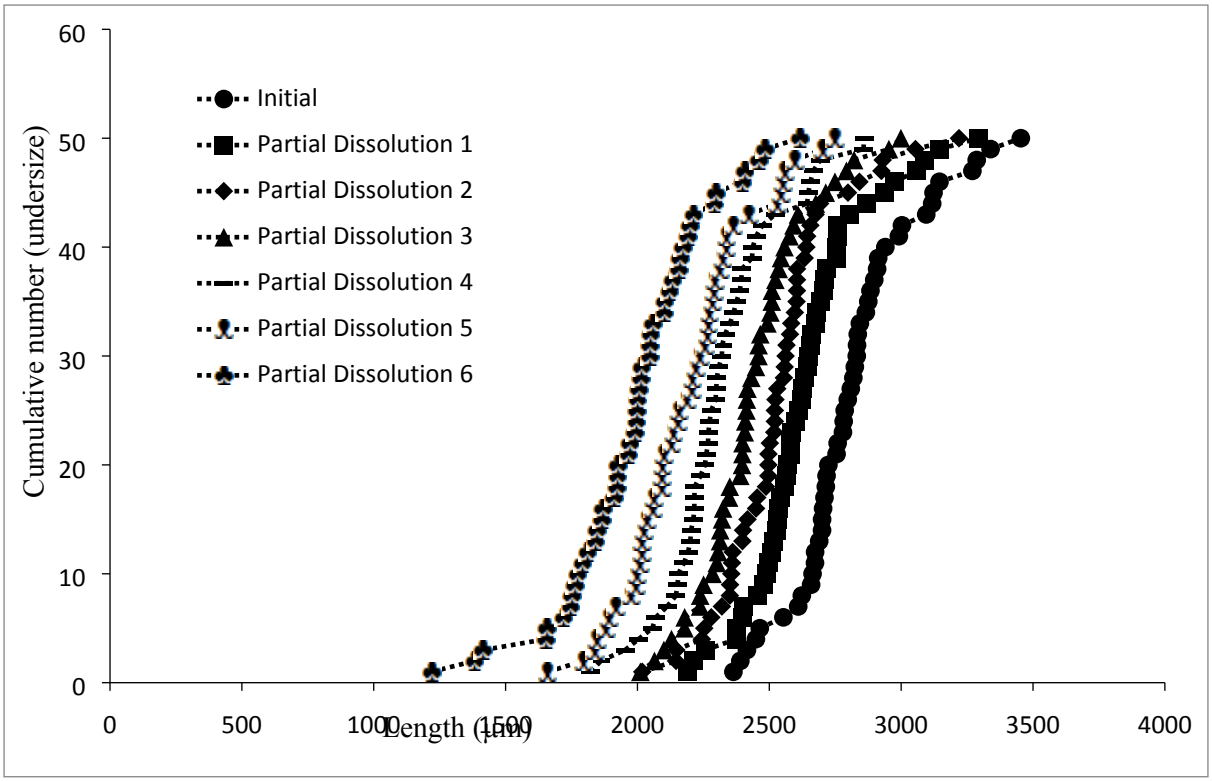

Fig. S35 Chart comparing particle length versus the ranking of each particle in a partial dissolution series of **1** doped with 5.0 mol % of **2**.

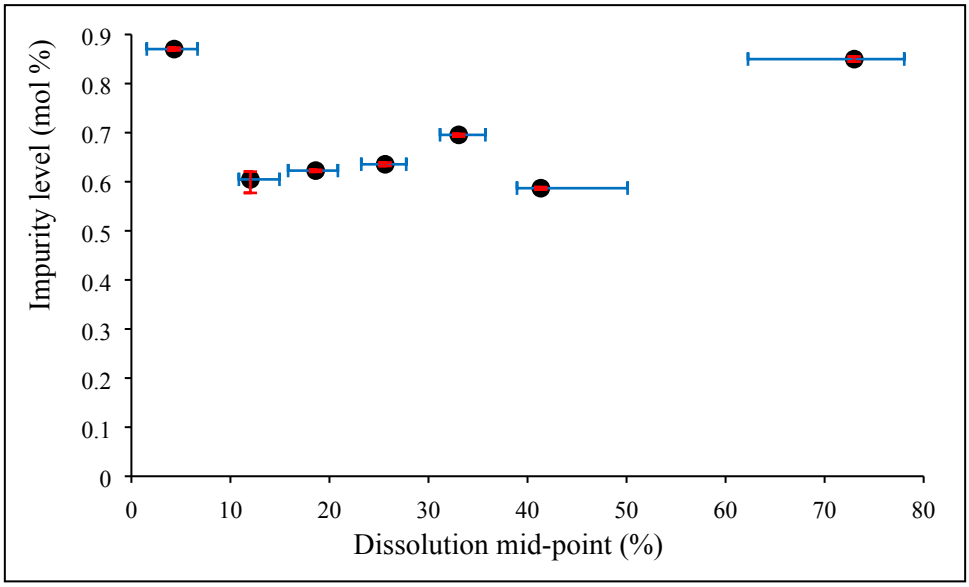

Fig. S36 Plot of percentage by HPLC of added impurity in crystals of compound **1** *vs.* the dissolution mid-point for the sample of crystals grown from solutions containing 5.0 mol % of additive **2**.

Table S2. Comparisons of parent batch average and weighted averages from stepwise dissolutions.

Entry	Additive	%additive in soln.	%additive in parent sample	Weighted% additive in dissolution sample*	Difference (%)
1	**2**	1.5	0.340 (0.06)	0.1664 (0.0014)	+0.18 (0.06)
2	**2**	2.0	0.442 (0.003)	0.3573 (0.0005)	+0.085 (0.003)
3	**2**	2.5	0.497 (0.017)	0.4054 (0.0011)	+0.091 (0.017)
4	**2**	3.0	0.630 (0.05)	0.4961 (0.0015)	+0.13 (0.05)
5	**2**	3.5	0.690 (0.015)	0.665 (0.005)	+0.025 (0.016)
6	**2**	4.0	0.838 (0.011)	0.7866 (0.0018)	+0.051 (0.011)
7	**2**	4.5	0.917 (0.012)	1.014 (0.012)	-0.097 (0.017)
8	**2**	5.0	0.980 (0.03)	0.739 (0.003)	+0.24 (0.03)
9	**3**	4.5	0.1867 (0.0005)	0.03995 (0.00015)	+0.1468 (0.0005)

*The weighted average was determined from the HPLC data using the following formula:

$$\sum_{i=1}^{n}\left(\frac{D_i}{\sum_{i=1}^{n} D_i}\right)\cdot R_i$$

where n is the number of partial dissolutions in a dissolution series, D_i is the number of moles of analytes dissolved in a partial dissolution step i, and R_i is the percentage of additive in the solution obtained from partial dissolution step i.

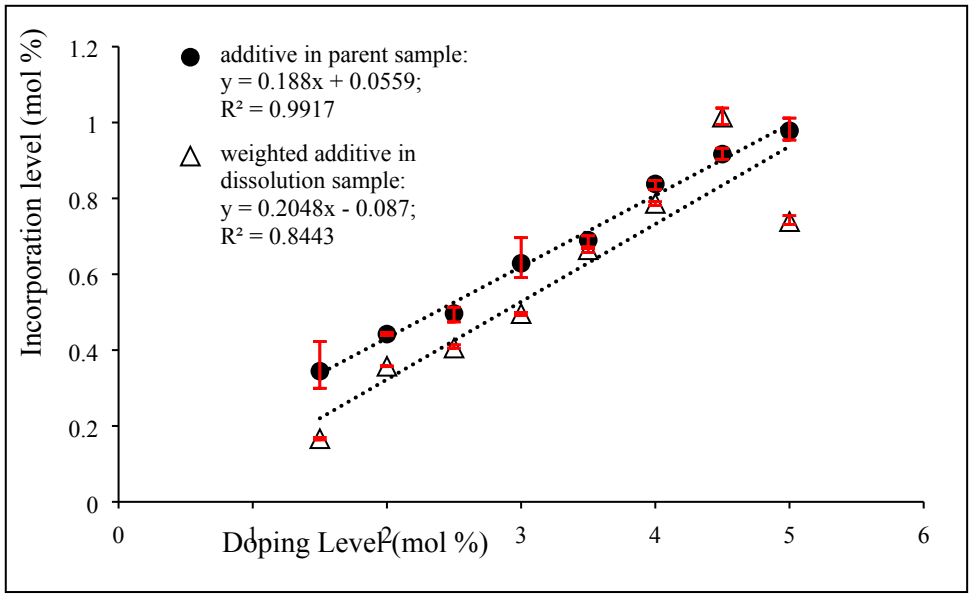

Fig. S37 Comparisons of parent batch average and weighted averages from stepwise dissolutions.

Table S3. Dissolution mid-points calculated for analysed 4.0 mol % **2**-doped **1** crystals from both observed measurements and 'theoretical' values.

Sample	Obs. Dissolution Area MdPt [%]	'Theor.' Dissolution Area MdPt [%]	Area MdPt Difference [%] [Obs. - Theor.]	Obs. Dissolution Length MdPt [%]	'Theor.' Dissolution Length MdPt [%]	Length MdPt Difference [%] [Obs. - Theor.]
Initial	5.0 (3.9)	3.4	1.6 (3.9)	2.71 (1.08)	1.73	0.98 (1.08)
PD1	12.5 (8.4)	10.3	2.2 (8.4)	6.8 (2.2)	5.3	1.5 (2.2)
PD2	18.9 (3.5)	17.5	1.4 (3.5)	10.3 (2.6)	9.2	1.1 (2.6)
PD3	26.84 (5.08)	25.01	1.83 (5.08)	15.05 (3.92)	13.43	1.62 (3.92)
PD4	34.6 (5.9)	32.9	1.7 (5.9)	20.2 (4.0)	18.1	2.1 (4.0)
PD5	46.7 (8.4)	41.4	5.3 (8.4)	26.7 (7.5)	23.5	3.2 (7.5)
PD6	77.4 (17.7)	72.9	4.5 (17.7)	65.3 (13.9)	63.2	2.1 (13.9)

References

1 S. Krakert, N. Ballav, M. Zharnikov and A. Terfort, *Phys. Chem. Chem. Phys.*, 2010, **12**, 507–515.